

Aus der Medizinischen Klinik und Poliklinik II
der Ludwig-Maximilians-Universität München
Direktor: Prof. Dr. med. Julia Mayerle

**Novel targets and therapeutic strategies for the treatment of
hepatocellular carcinoma (HCC)**

Dissertation
zum Erwerb des Doktorgrades der Medizin
an der Medizinischen Fakultät der
Ludwig-Maximilians-Universität zu München

vorgelegt von

Liangtao Ye

aus Guangdong Provinz, V. R. China

2019

Mit Genehmigung der Medizinischen Fakultät
der Universität München

Berichterstatter: Priv. Doz. Dr. med. Enrico N. De Toni

Mitberichterstatter: Priv. Doz. Dr. med. Susanna Müller
Priv. Doz. Dr. med. Dr. sci. nat. Fabian
Hauck

Dekan: Prof. Dr. med. dent. Reinhard Hickel

Tag der mündlichen Prüfung: 06. 06. 2019

Eidesstattliche Versicherung

Liangtao Ye

Ich erkläre hiermit an Eides statt, dass ich die vorliegende Dissertation mit dem Thema

Novel targets and therapeutic strategies for the treatment of hepatocellular carcinoma (HCC)

selbständig verfasst, mich außer der angegebenen keiner weiteren Hilfsmittel bedient und alle Erkenntnisse, die aus dem Schrifttum ganz oder annähernd übernommen sind, als solche kenntlich gemacht und nach ihrer Herkunft unter Bezeichnung der Fundstelle einzeln nachgewiesen habe.

Ich erkläre des Weiteren, dass die hier vorgelegte Dissertation nicht in gleicher oder in ähnlicher Form bei einer anderen Stelle zur Erlangung eines akademischen Grades eingereicht wurde.

Munich, 07. 06. 2019

Ort, Datum

Liangtao Ye

Unterschrift Doktorand

TABLE OF CONTENTS

INTRODUCTION 8

The PI3K inhibitor copanlisib synergizes with sorafenib to induce cell death in hepatocellular carcinoma (HCC)

ABSTRACT 10

ZUSAMMENFASSUNG 11

INTRODUCTION 13

MATERIALS & METHODS 15

 Cell lines and reagents 15

 Cell proliferation assays 15

 Colony formation assay 16

 Apoptosis and cell cycle assays 16

 Western blot 16

 Statistical analysis 17

RESULTS 18

 Copanlisib exerts a potent anti-proliferative effect as single agent in HCC cells 18

 Copanlisib causes G1 cell cycle arrest and downregulation of cyclin B1 and D1 18

 Copanlisib synergizes with sorafenib by counteracting sorafenib-induced activation of AKT 19

Co-treatment with copanlisib and sorafenib enhances apoptotic cell death in a caspase-dependent way.....	20
DISCUSSION	22
Conclusion	24
FIGURES	25
Prognostic significance and functional relevance of olfactomedin 4 (OLFM4) in the development of hepatocellular carcinoma	
ABSTRACT	39
ZUSAMMENFASSUNG	41
INTRODUCTION	43
MATERIALS & METHODS	45
Patients and pathologic material.....	45
Immunohistochemical staining.....	45
Histologic assessment of tumours and surrounding non-tumour tissues	46
Cell culture	46
Human tissue for isolation of primary human hepatocytes.....	46
Western blot.....	47
siRNA interference.....	48
Immunofluorescence.....	48
Flow cytometry.....	49

Proliferation assay.....	49
Scratch assay.....	49
Migration and invasion assay.....	50
Cancer genome atlas analyses.....	50
Statistical analysis.....	50
RESULTS	51
Patients and clinicopathological parameters.....	51
Immunohistochemical staining for OLFM4 in HCC cells and in hepatocytes from surrounding non-tumour tissues.....	51
Correlation of OLFM4 staining with clinicopathologic features of tumour tissues and non-tumour surrounding tissues.....	52
Prognostic significance of OLFM4 staining in patients undergoing liver resection.....	52
OLFM4 silencing suppresses cell migration and invasion, and causes cell cycle arrest <i>in vitro</i>	54
DISCUSSION	56
Staining, localization and prognostic significance of OLFM4 in tumours versus surrounding non-tumour tissues.....	56
Clinical-pathologic correlations of OLFM4 staining and functional assessment of OLFM4 <i>in vitro</i>	57
Possible clinical consequences of OLFM4 expression in liver cancer cells.....	58

Summary.....	59
FIGURES	60
TABLES	71
REFERENCES	79
LIST OF ABBREVIATIONS	86
ACKNOWLEDGMENT	88
CURRICULUM VITAE	89

INTRODUCTION

Liver cancer is a leading cause of cancer-related mortality worldwide and accounts for more than 800.000 deaths per year. Hepatocellular carcinoma (HCC) is a common cancer with high lethality, which is diagnosed most often at advanced stages when surgical or local treatment options are not possible. For the treatment of advanced HCC, sorafenib has been the only approved systemic treatment for nearly 10 years. Lately however, a number of additional compounds targeting tumour-specific signalling pathways, such as regorafenib, lenvatinib, and cabozantinib, and most recently, ramucirumab, provided positive results in phase-3 clinical trials. In addition, the approval of nivolumab as second-line treatment revealed the importance of the immune response in determining the development in HCC and set the stage for extensive clinical research with these agents. These new therapeutic options for HCC have significantly prolonged the life expectancy in patients with advanced-stage disease and collectively provided evidence that targeted therapy in different lines of treatment is a feasible strategy also for HCC. Nevertheless, a great individual variability in clinical benefits in response to these agents can be observed, and prognosis remains extremely poor in the majority of patients not responding to the treatments.

By the two presented research projects, we aimed at assessing new therapeutic targets and possible therapeutic strategies for the treatment of HCC.

In the first project, which was previously published in the form of an abstract ¹, we explored the possibility of enhancing the therapeutic potential of sorafenib by its combination with the novel and clinically viable PI3K-Akt-Tor inhibitor copanlisib. To this regard, we found that copanlisib possesses potent anticancer activity as single agent and acts synergistically in combination with sorafenib in

human HCC, hereby representing a rational potential therapeutic option for advanced HCC.

In the second project, which was also presented and published as an abstract ², we investigated the role of olfactomedin 4 (OLFM4), a glycoprotein predominantly expressed in bone marrow and gastrointestinal tract, in the pathogenesis of HCC. By performing immunohistochemical staining in human HCC tissues and functional *in vitro* assays of Huh7 and HepG2 cell lines, we provided the first report on a possible role of this molecule in determining the development of HCC by showing that increased expression of OLFM4 is a common event in the pathogenesis of this tumor with independent prognostic significance.

Our preclinical results from these two studies, which are presented in the form of the two different manuscripts about to be submitted or published, warrant further investigation of PI3K-Akt-Tor signalling as a mechanism of cancer development and chemoresistance during HCC treatment, as well as of the role played by OLFM4 in determining invasion and metastasis in this tumor.

The PI3K inhibitor copanlisib synergizes with sorafenib to induce cell death in hepatocellular carcinoma (HCC)**ABSTRACT**

Background: Sorafenib, a multikinase inhibitor targeting the Ras/Raf/MAPK and VEGF signaling pathways is an established treatment option for patients with advanced-stage hepatocellular carcinoma (HCC); however, despite its clinical benefit, chemoresistance and disease progression eventually occur almost invariably during treatment. Activation of the PI3K/AKT pathway plays a role in the pathogenesis of HCC and may contribute to determine resistance to sorafenib. We thus evaluated *in vitro* the effects of the combination of sorafenib and copanlisib, a PI3K inhibitor recently approved for clinical use.

Methods: The effects of copanlisib alone and in combination with sorafenib were assessed in several HCC cell lines by proliferation and colony formation assays, FACS analyses, and western blot. In addition, sorafenib-resistant cell clones were used.

Results: Copanlisib strongly reduced cell viability and colony formation in different native and sorafenib-resistant HCC cell lines by affecting cyclin D1/CDK4/6 signaling and causing cell cycle arrest. Elevation of p-AKT was observed upon incubation with sorafenib and was consistently found in 6 different unstimulated sorafenib-resistant cell clones. Copanlisib counteracted sorafenib-induced phosphorylation of p-AKT and synergistically potentiated its antineoplastic effect.

Conclusion: Copanlisib shows potent anticancer activity as single-agent and acts synergistically in combination with sorafenib in human HCC. Combination of sorafenib with copanlisib represents a rational potential therapeutic option for advanced HCC.

Der PI3K-Inhibitor Copanlisib synergisiert mit Sorafenib, um den Zelltod bei einem hepatozellulären Karzinom (HCC) zu induzieren

ZUSAMMENFASSUNG

Hintergrund: Die Therapie mit Sorafenib, einem gegen die Ras/Raf/MAPK- und VEGF-Signalwege gerichteter Multikinase-Inhibitor, ist eine etablierte Behandlungsoption für Patienten mit fortgeschrittenem hepatozellulärem Karzinom (HCC). Trotz des klinischen Nutzens treten unter der Behandlung fast immer eine Chemoresistenz und ein Fortschreiten der Krankheit auf. Die Aktivierung des PI3K/AKT-Signalwegs spielt eine Rolle in der Pathogenese des HCCs und kann zur Entstehung einer Resistenz gegen Sorafenib beitragen. Daher haben wir die Wirkung von Sorafenib in Kombination mit Copanlisib, einem kürzlich für die klinische Anwendung zugelassenen PI3K-Inhibitor, *in vitro* untersucht.

Methoden: Die Effekte von Copanlisib allein und in Kombination mit Sorafenib wurden in mehreren HCC-Zelllinien mittels Proliferations- und Koloniebildungsassays, FACS-Analysen und Western Blot untersucht. Zusätzlich wurden Sorafenib-resistente Zellklone verwendet.

Ergebnisse: Copanlisib reduzierte die Zellebensfähigkeit und Koloniebildung in verschiedenen nativen und Sorafenib-resistenten HCC-Zelllinien stark, indem es den Cyclin D1/CDK4/6 Signalweg beeinflusste und einen Zellzyklusstillstand verursachte. Eine Erhöhung von p-AKT wurde nach Behandlung mit Sorafenib beobachtet und konnte in sechs verschiedenen nicht stimulierten Sorafenib-resistenten Zellklonen übereinstimmend gefunden werden. Copanlisib wirkt der Sorafenib-induzierten Phosphorylierung von p-AKT entgegen und potenziert synergistisch dessen antineoplastischen Effekt.

Schlussfolgerung: Copanlisib zeigt eine starke antitumoröse Akitvität als Einzelwirkstoff und wirkt in Kombination mit Sorafenib im humanen HCC Zelllinien synergistisch. Die Kombination von Sorafenib mit Copanlisib stellt eine rationale mögliche therapeutische Option für das fortgeschrittene HCC dar.

INTRODUCTION

Hepatocellular carcinoma (HCC) is the second cancer-related cause of death worldwide accounting for about 800,000 deaths every year and its incidence is expected to progressively increase in the future ³⁻⁵. The improvement of local and locoregional therapies, the definition of selection criteria for liver transplantation, and the implementation of screening programs for early diagnosis have contributed to the amelioration of survival of HCC patients ⁶. In addition, the advent of sorafenib ⁷ and the recent positive results of clinical trials investigating new compounds such as regorafenib ⁸, lenvatinib ⁹, nivolumab ¹⁰ and, most recently, cabozantinib ¹¹, shows that the sequential employment of compounds targeting different signaling pathways is a therapeutic strategy applicable to the treatment of HCC, promising to further ameliorate the life expectancy of patients with advanced stage tumors. Future treatment schemas will thus likely consist of the combination of different kinase inhibitors simultaneously targeting different intracellular signaling pathways to overcome chemoresistance to single treatment regimens and/or their combination with immune checkpoint inhibitors ¹².

Sorafenib is a multikinase inhibitor which influences a number of different signalling pathways, including the Ras/Raf/MAPK pathway, VEGF- and PDGF-signalling, hereby affecting different aspects of cell biology including proliferation, apoptosis and angiogenesis ¹³. Unfortunately, due to both the molecular heterogeneity of HCC and the broad spectrum of kinase inhibition peculiar of sorafenib, in spite of substantial efforts, no reliable predictors of response to this drug could be found yet, and the precise mechanism of action of sorafenib remains to be precisely elucidated. Nevertheless, the observation that recurrent molecular changes occur in consequence of sorafenib treatment (including increase of c-MET ¹⁴ and the activation of the phosphatidylinositol-3-

kinase (PI3K)-serine/threonine kinase (AKT)-mammalian target of rapamycin (mTOR) signalling pathway^{15,16}) indicates that concomitant inhibition of these signalling pathways can be exploited to overcome resistance to sorafenib. The compensatory activation of these signalling pathways is in keep with the significance of c-MET and PI3K-Akt-Tor signalling in the pathogenesis of HCC recently highlighted by extensive genetic investigation of this tumor^{17,18}.

Copanlisib (BAY 80-6946) is a novel PI3K inhibitor which demonstrated effectiveness in various tumour entities in preclinical models¹⁹⁻²² and is currently undergoing extensive clinical investigation. Most recently, copanlisib was granted accelerated approval for therapy of follicular lymphoma recurrence. Here, we aimed at assessing the potential antineoplastic effect of copanlisib in HCC cell lines and its potential as a sensitizer to the antineoplastic effect of sorafenib in a preclinical model.

MATERIALS AND METHODS

Cell lines and reagents

Huh7, HepG2, PLCPRF5, Chang cells were cultured in Dulbecco's Modified Eagle's Medium (DMEM) and Hep3B cells were cultured in Minimum Essential Medium Eagle (MEM) (Sigma Aldrich, Munich, Germany) with 10% fetal bovine serum (Biochrom GmbH, Berlin, Germany), 1% penicillin-streptomycin (Sigma Aldrich, Munich, Germany). Cells were maintained in 5% CO₂ at 37 °C. Copanlisib (BAY 80-6946, Selleckchem, Munich, Germany) and sorafenib (Selleckchem, Munich, Germany) were stored at -20°C and dissolved in 100% dimethyl sulfoxide (DMSO) at a stock concentration of 5 mMol and 43 mMol, respectively. Two sorafenib resistant sublines were established from Huh7 and HepG2 cells, termed sorafenib-resistant Huh7 (Huh7-SR) and sorafenib-resistant-HepG2 (HepG2-SR), by incubation with increasing doses of sorafenib (2 µM, 4 µM, and 6 µM) for at least eight months. Authentication of cell lines was conducted by Leibniz Institute DSMZ-German Collection of Microorganisms and Cell Cultures.

Cell proliferation assays

1,000 to 1,500 cells were seeded in 96-well plates, cultured overnight, and then incubated in the presence of various concentrations of copanlisib and/or sorafenib. After 6 days, cells were washed with PBS and underwent osmotic lysis in 100 µl ddH₂O for 45 minutes at 37 °C. 0.2% Sybr green (Lonza, Rockland, ME, USA) was added to each well, fluorescence was measured (GloMax-Multi+Detection System with Instinct Software, Promega, USA) and proliferation index was calculated as a ratio to untreated samples. Three independent experiments were performed per agent, with each data point reflecting triplicate wells. Error bars represented standard deviation of the mean

(SD) from three experiments. Data were analysed by using CompuSyn (Biosoft, Ferhuson, MO, USA) to calculate the IC₅₀ to determine the IC₅₀ of the assessed drugs. The same software was used was used to draw isobolograms and calculate the Chou-Talalay combination index (CI), an established method to calculate drug-interaction as previously described²³. Combination index values of <1, 1, and >1 indicated synergistic, additive, and antagonistic effects, respectively.

Colony formation assay

5,000 cells were seeded in 6-wells plates. After overnight incubation, cells were exposed to copanlisib for 48 hours. Fresh medium was replaced regularly and the plates were maintained at 37 °C for three weeks. Colonies were counted after fixation in 9% paraformaldehyde and staining with crystal violet for 30 minutes (Sigma, St. Louis, MO, USA).

Apoptosis and cell cycle assays

8.0×10^4 to 1.5×10^5 cells were seeded in 6-well plates. After overnight incubation and incubation with the respective agents, propidium iodide (PI) staining and fluorescence-activated cell sorting (FACS - Accuri C6 flow cytometer, BD Biosciences San Jose, CA USA) were performed to assess the fraction of apoptotic cells as determined by the sub-diploid DNA content (Sub-G1). In addition, apoptosis was assessed by Hoechst staining and fluorescence microscopy (Zeiss, Jena, Germany).

Western blot

Equal amount of proteins in each sample was loaded on 10/12% SDS-PAGE gels and separated for 25 minutes at 80 V and for 80 minutes at 120 V, then transferred onto PVDF membranes (EMD Millipore Corporation, Billerica, MA,

USA). After blocking for 1 hour in TBST (tris-buffered saline with Tween-20) containing 5% milk or 5% bovine serum albumin, membranes were incubated overnight at 4°C with the following primary antibodies: p-AKT (S473), AKT, β -actin, Caspase-3, Caspase-8, Caspase-9, Cyclin B1, Cyclin D1, p53, p21, CDK4, CDK6, Bad, Bax, Bak, Bcl-2, Bcl-xL (Cell Signaling Technology, USA) and Bid (FL-195; Santa Cruz, Germany). Subsequently, the membrane was probed with horseradish-peroxidase conjugated secondary anti-rabbit or -mouse IgG antibodies (GE Healthcare UK Limited) for 2 hours at room temperature at concentrations of 1:10,000. The bands were visualized by SuperSignal West Pico Chemiluminescent Substrate (Thermo Scientific, Schwerte, Germany) and photographed with an image acquisition system (ECL ChemoCam Imager, Intas GmbH, Germany).

Statistical analysis

Data were analysed by SPSS version 22.0 (SPSS Inc, IL USA). Results were shown as mean \pm standard deviation (SD) of at least three independent experiments and statistical difference were assessed by Student's t-test and one-way analysis of variance (ANOVA) test followed by LSD method. Statistical significance was defined by P values < 0.05 ; \neq , $P < 0.05$; O, $P < 0.01$; *, $P < 0.001$. The combination index was determined as described above ²³.

RESULTS

Copanlisib exerts a potent anti-proliferative effect as single agent in HCC cells.

The effect of copanlisib on cell viability was assessed in 5 HCC cell lines exhibiting different baseline levels of p-AKT expression (**Fig. 1A**). As shown in **Fig. 1B**, the effect of copanlisib on p-AKT was readily observable after one-hour incubation at the concentration of 100 nM. Copanlisib dose-dependently inhibited cell growth *in vitro* in clinical concentration-range regardless of baseline levels of p-AKT, hereby showing higher potency in Huh7 and HepG2 ($IC_{50}=47.9$ and 31.6 nM, respectively) vs Hep3B, PLCPRF5 or Chang cells ($IC_{50}=72.4$, 283 nM, and $IC_{50}=442$ nM respectively; **Fig. 1C**). These results were clearly confirmed by clonogenicity assays, showing a dose-dependent reduction in number and size of colonies in Huh7 and HepG2 cells upon incubation with copanlisib (**Fig. 1D-E**).

Copanlisib causes G1 cell cycle arrest and downregulation of cyclin B1 and D1.

Since copanlisib was previously shown to cause apoptosis by inhibiting the antiapoptotic protein Bcl-xL in breast cancer cells ²⁴, apoptosis and cell cycle were assessed to determine their respective contribution to its antineoplastic effect in HCC cells. Surprisingly, we found only little or quantitatively negligible apoptosis, as shown by the time-kinetic of sub-G1 events at different time points until 72 hours after addition of copanlisib at the concentrations of 100 and 200 nM (**Fig. 2A-C**). This was confirmed by the absence of typical microscopic features of apoptosis, like chromatin condensation and nuclear fragmentation at Hoechst staining (**Fig. 2D**). Instead, incubation with copanlisib

for up to 72 hours caused a clear, dose- and time- dependent G1 cell cycle arrest, along with a corresponding decrease of the S and G2/M phases of cell cycle (**Fig. 2E-G**). Correspondingly, as key modulators of cell death and cell cycle were assessed, no caspase cleavage could be detected (**Fig. 3**). Instead, cell cycle arrest was accompanied by a significant reduction of cyclin B1 and cyclin D1 24 to 72 hours after addition of copanlisib. Concomitantly, an increase of both p53 and p21 and a decrease of CDK4 and CDK6 were observed (**Fig. 3**). These data point to the fact that copanlisib used as single agent affects the viability of HCC cells mainly by inducing cell cycle arrest by downregulating CDK4/6 and cyclin D1, which are downstream targets of AKT, but only marginally effects apoptosis.

Copanlisib synergizes with sorafenib by counteracting sorafenib-induced activation of AKT.

Since sorafenib-induced increase of AKT phosphorylation is thought to represent a mechanism of chemoresistance counteracting the antineoplastic effect of sorafenib ^{16,25,26}, we assessed the effect of combined sorafenib and copanlisib in HCC cells. As expected, sorafenib strongly diminished cell viability alone hereby causing increased expression and cleavage of procaspase 3 and 9 (**Fig. 4**). In the same time, however, incubation with sorafenib induced increase of p-AKT, cyclin B1 and cyclin D1. However, this effect could be reversed by co-incubation with copanlisib. In addition, co-administration of sorafenib and copanlisib increased caspase cleavage. The antineoplastic interaction between sorafenib and copanlisib was confirmed by CI and isobologram blots showing that copanlisib and sorafenib synergize to determine the loss of cell viability in Huh7 and HepG2 cells (**Fig. 4B-E**). Altogether these

data suggest that sorafenib-mediated activation of AKT and cyclin D1 might represent a mechanism of resistance limiting the antineoplastic potential of sorafenib.

To confirm these findings, we established several cell lines with acquired resistance to sorafenib by long-term exposure to increasing concentrations of this agent. As expected, such Huh7- and HepG2-derived cells lines were less sensitive to sorafenib in comparison to their wild-type counterpart (**Fig. 5A-B**). In addition, they exhibited increased levels of phosphorylated AKT, of cyclin D1, of CDK4 and CDK6 (**Fig. 5C**), an effect which could be counteracted by copanlisib (**Fig. 5D**). Correspondingly, as shown by viability experiments, copanlisib restored sorafenib sensitivity in sorafenib-resistant cells (**Fig. 5E-F**).

Taken together, these results indicate that increase of AKT is not only triggered in response to sorafenib but also represents a mechanism of acquired resistance developing after long-term exposure to this agent. AKT inhibition by copanlisib counteracts this mechanism of resistance hereby sensitizing cancer cells to sorafenib.

Co-treatment with copanlisib and sorafenib increases apoptosis by a caspase-dependent mechanism.

To investigate the mechanisms underlying the synergistic interaction between copanlisib and sorafenib in Huh7 and HepG2 cells, we examined the effect of their combination in determining cell cycle and apoptosis. In agreement with the observed increase in caspase cleavage caused by co-stimulation with both agents (**Fig. 4A**), a synergistic increase of apoptosis (**Fig. 6A-C**) and an additive increase of cell cycle arrest were observed (**Fig. 7A-C**). At molecular level, western blot analysis showed that the combined substances cause an increase of

the proapoptotic proteins bad, bid, bax, and bak and a decrease of the antiapoptotic molecules Bcl-2 and Bcl-xL (**Fig. 8A**).

DISCUSSION

Derangement of the PI3K signaling pathway is one of the most common events in cancer development ^{27,28} and is thought to play a role in the development of approximately 50% of HCC ¹⁷. Sorafenib, a standard first-line treatment option for HCC, is known to possess a broad spectrum of kinase inhibition, but has little effect on the activity of the PI3K-Akt-Tor signaling, a pathway which, as recently proposed ^{29,30} might represent a mechanism of acquired resistance to this agent.

Copanlisib is a newly developed pan-PI3K inhibitor which has most recently been approved for the treatment of relapsed follicular lymphoma ³¹ and is undergoing clinical experimentation for the treatment of indolent or aggressive NHL ³². In addition, copanlisib is being assessed for the treatment of solid tumors in preclinical studies ^{19,22,24} and in early-phase clinical trials showing signs of effectiveness and acceptable toxicity ^{33,34}. The availability of this agent for clinical use represented the rationale for assessing its combined effect with sorafenib for treatment of HCC.

In our model, copanlisib showed remarkable antiproliferative properties in different HCC cell lines independently of their basal expression of AKT. Previous investigation in breast cancer cells had shown that copanlisib causes apoptosis by down-regulating the expression of the antiapoptotic protein Bcl-xL ²⁴. In contrast, our findings show that copanlisib suppresses tumor growth in HCC cells mainly by triggering a G1 cell cycle arrest by inhibiting the cyclin D1/CDK4/CDK6 axis (**Fig. 8B**), without causing apoptosis (**Fig. 3**). Cyclin D1, CDK4 and CDK6 are regulated by the PI3K-Akt-Tor signalling pathway and control the progression from the G1 to the G2 phase of cell cycle by phosphorylating the tumour suppressor Rb , which in turn causes the activation

of the transcription factor E2F³⁵. Extensive efforts to characterize the mutational landscape of HCC by exome sequencing recently conducted by the group of Zuckmann-Rossi and colleagues has revealed that amplification of cyclin D1 is one of the most frequent events during HCC development and is independently associated with a poor prognosis¹⁷. The frequent activation of the PI3K-Akt-Tor signalling and amplification of cyclin D1 in HCC corroborate the rationale for assessing copanlisib as a treatment option in patients with advanced HCC.

In addition to its antiproliferative properties as single agent, copanlisib also synergistically potentiates the effect of sorafenib, which is consistent with the notion that the activation of PI3K serves as mechanism of escape from the inhibition of Ras-Raf-MAPK signalling. We correspondingly found that p-AKT as well as cyclin-B1, -D1 and CDK4/6 were increased by sorafenib, an effect which could be completely abrogated by copanlisib. Our observations are in accordance with previous studies showing that interruption of PI3K/AKT signaling sensitizes tumor cells to sorafenib-induced apoptosis¹⁶ and with the fact that we consistently found high basal levels of p-AKT, CDK4/6 and cyclin D1 in cell lines with acquired resistance to sorafenib.

Interestingly, we observed that the mechanisms underlying the effects of the combined agents were different those observed with copanlisib alone. Copanlisib had little effect on apoptosis, which was instead remarkably increased by the combination of both agents. This proapoptotic effect was caused by the activation of the intrinsic signaling pathway, in particular owing to the profound down-regulation of the antiapoptotic molecules Bcl-2 and Bcl-xL, an effect which was previously suggested as mechanism of action of copanlisib in breast cancer cells²⁴.

While our results suggest the possibility that copanlisib could be used as treatment option for patients with advanced HCC alone or in combination with sorafenib, copanlisib might also be used in combination with other anticancer agents, comprising immune checkpoint inhibitors. The association of immune checkpoint inhibitors with kinase inhibitors seems to represent a promising therapeutic approach, as exemplified by a recent early-stage trial with combined lenvatinib and pembrolizumab ³⁶. Since clinical evidence was provided on the efficacy of combined mTOR-inhibitors and PD-1/PD-L1 blocking agents in HCC and metastatic renal cell carcinoma ^{37,38}, copanlisib could be used in combination with immune checkpoint inhibitors to potentiate the effect of these agents.

Conclusion

In summary, we highlight the role of PI3K-Akt-Tor signalling activation in inducing resistance to sorafenib, and shed light on the mechanism of action underlying the antineoplastic effects of copanlisib and its synergistic interaction with sorafenib. We suggest that copanlisib is considered as a potential treatment option for HCC alone or in combination with sorafenib.

FIGURES

Figure 1

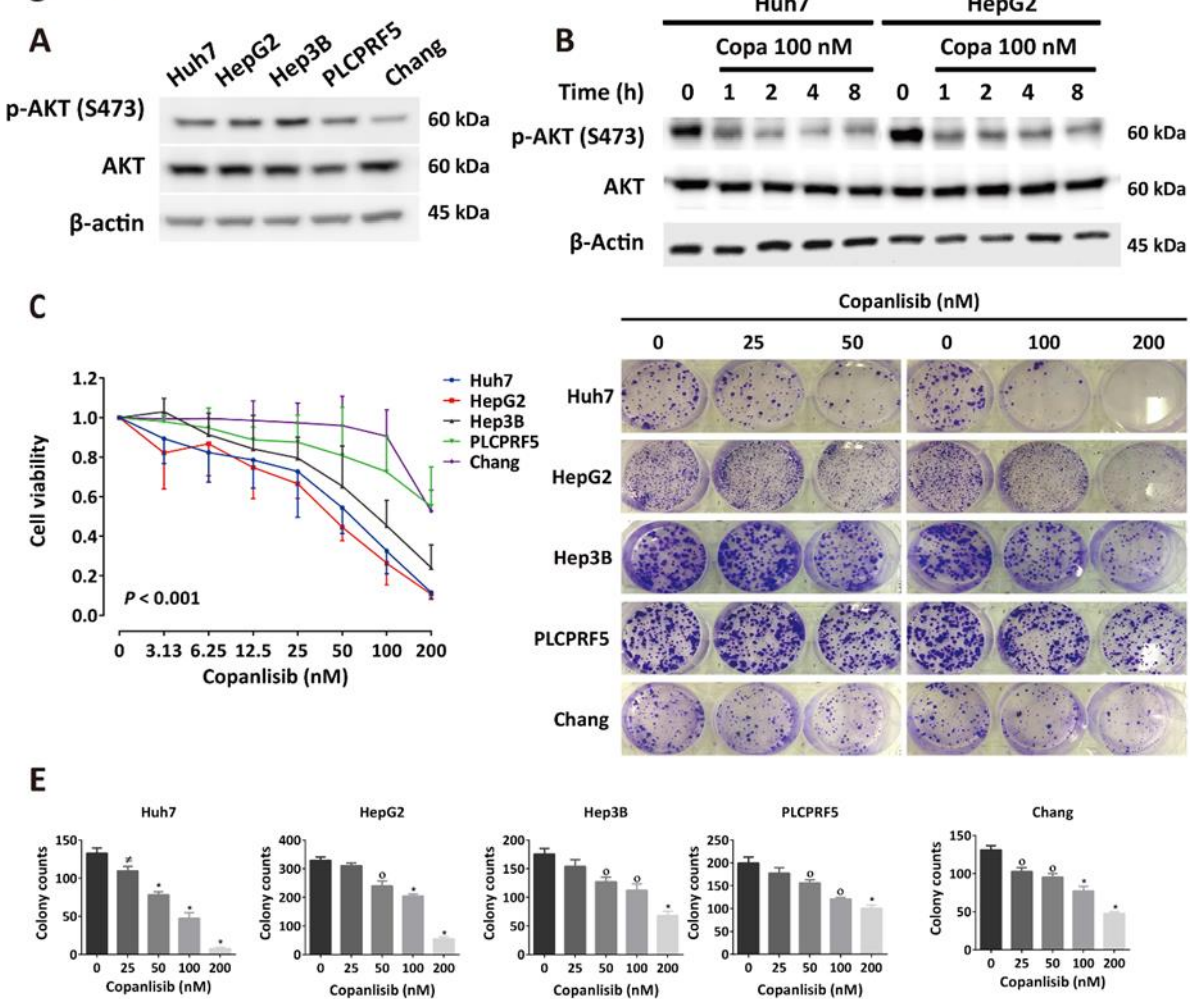


Fig. 1. Copanlisib affects cell viability and colony forming capability. **A.** Baseline levels of p-AKT expression in the indicated cell lines. **B.** Effect of copanlisib (copa) at the concentration of 100 nM on p-AKT. **C.** Changes in cell viability expressed as ratio to control-treated cells at different concentrations of copanlisib. **D.** Representative pictures of colony-formation of Huh7 and HepG2 cells and **(E)** colony count, after incubation with the indicated concentrations. Results are representative of three independent experiments. Error bars represent mean \pm standard deviation (SD).

Figure 2

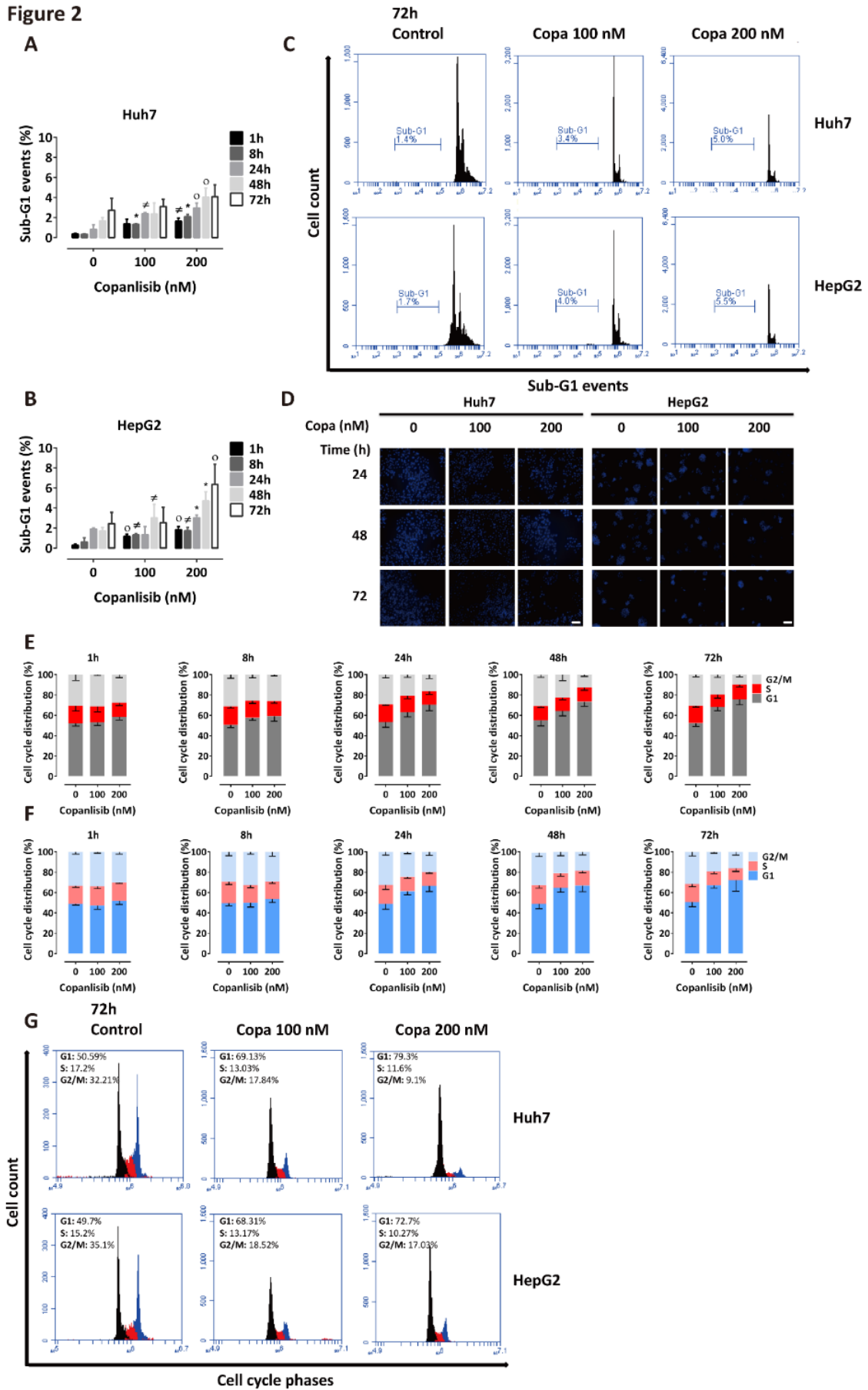


Fig. 2. Copanlisib causes a G1 cell cycle arrest. Sub-G1 events upon incubation with copanlisib at the concentrations of 100 and 200 nM in Huh7 (A) and HepG2 (B) cells showing marginal apoptosis; typical FACS pattern of sub-G1 cell fraction (C) and Hoechst staining (D) in these cell lines. Cell cycle analysis after incubation with copanlisib (copa) at the indicated concentrations and time points in Huh7 (E) and HepG2 (F) cells and respective representative features at FACS analysis (G). Reproducible results were obtained in at least three independent experiments. Error bars represent mean \pm SD. \neq : $P < 0.05$; O: $P < 0.01$; *: $P < 0.001$, by independent sample t-test vs. untreated controls. In these experiments, to rule out the possibility that the observed lack of apoptosis could be due to diminishing effectiveness of copanlisib during incubation, fresh medium containing copanlisib at the appropriate concentrations was replaced every day.

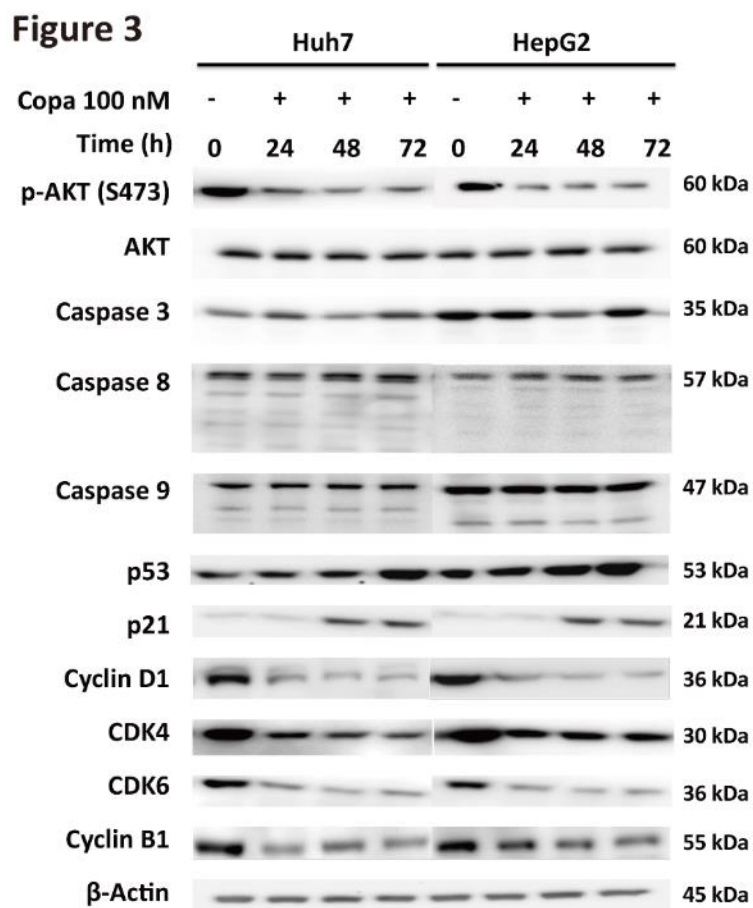


Fig. 3. Copanlisib triggers G1 cell cycle arrest by down-regulating cyclin B1 and D1. Immunoblot analyses of different regulators of apoptosis and cell cycle after incubation with

copanlisib (copa) at the concentration of 100 nM at the indicated time points. Three independent repeats.

Figure 4

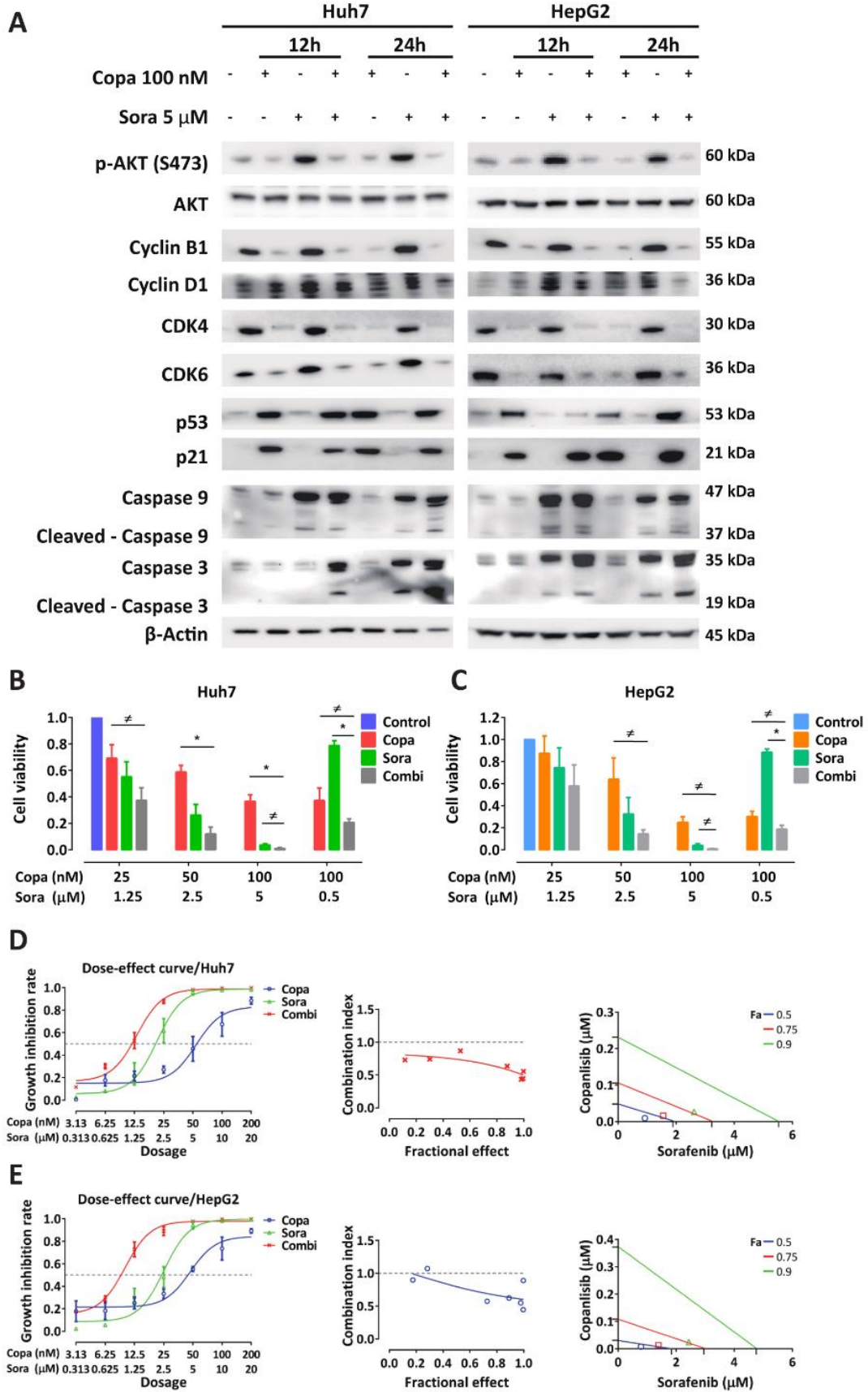


Fig. 4. Copanlisib synergizes with sorafenib to determine loss of cell viability by counteracting sorafenib-induced PI3K/AKT activation. **A.** Western Blot analysis of Huh7 and HepG2 after incubation with copanlisib and/or sorafenib at the indicated concentrations. **B. C.** Synergistic interaction between sorafenib and copanlisib in Huh7 (**B**) and HepG2 cells (**C**) as determined by cell viability. CI values of <1, 1, and >1 indicate synergistic, additive, and antagonistic effects, respectively (Copa: copanlisib; Sora: sorafenib; Combi: combination of both substances). **D.** Dose-effect relationship of copanlisib, sorafenib, and their combination (constant ratio of 1: 100) on growth inhibition of Huh7 cells (left panel). The combination index (CI) values and fraction affected (Fa) for each dose were used to generate the Fa-CI plot (middle panel) and isobologram blots (right panel). Panels of figure **E** represent for HepG2 the same information provided Huh7 cells. For viability assays cells were incubated with the indicated concentrations of copanlisib, sorafenib and their combination for six days. All *in vitro* assays were carried out on three independent experiments. Error bars represent mean \pm SD. \neq , $P < 0.05$; O, $P < 0.01$; *, $P < 0.001$, by independent sample t-test compared with untreated control, respectively.

Figure 5

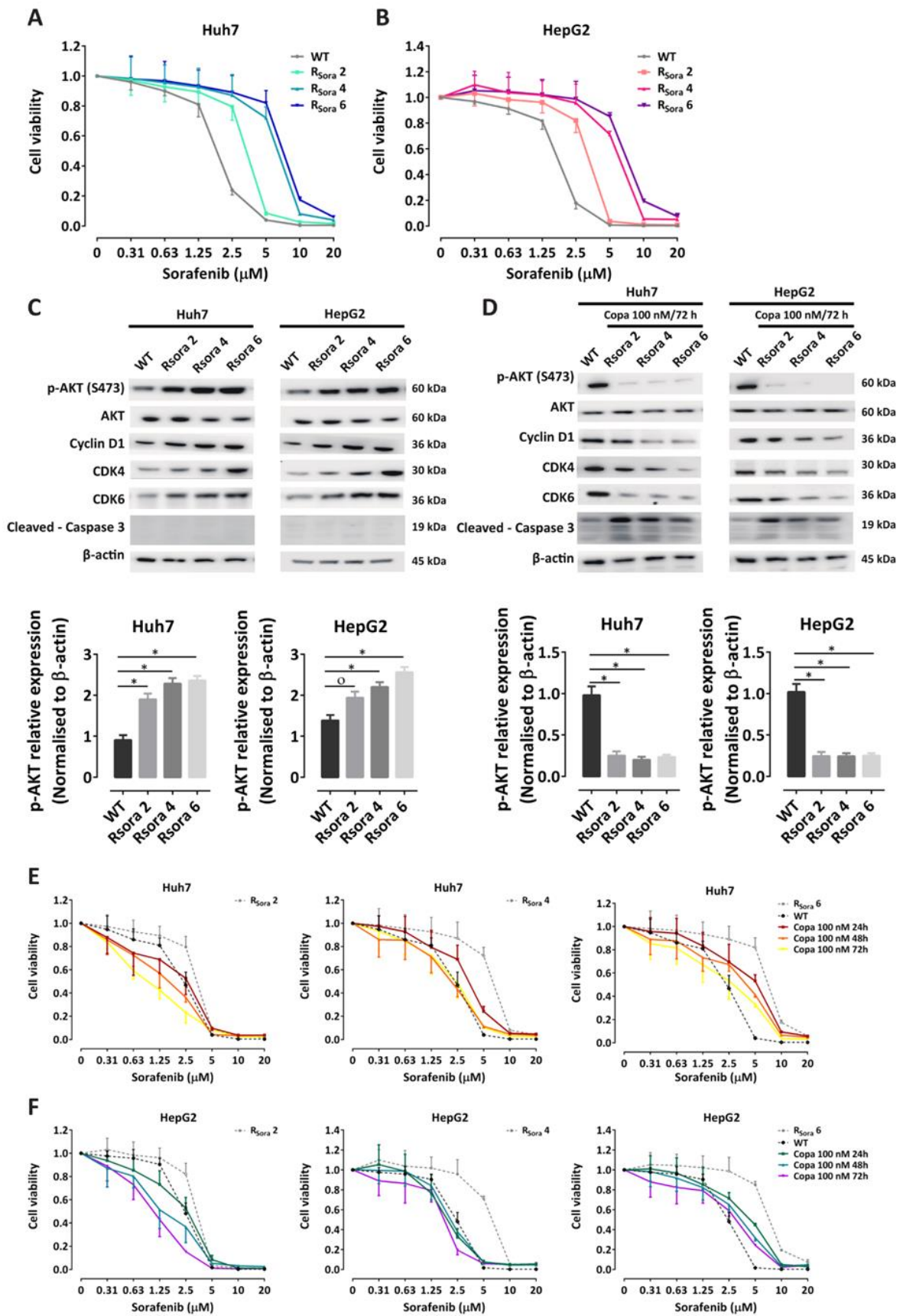


Fig. 5. Copanlisib restores the sensitivity of sorafenib-resistant Huh7 and HepG2 cell lines to sorafenib. **A. B.** Viability assay after incubation with sorafenib in wild type (WT) Huh7 and HepG2 cells and in cell lines which acquired resistance to sorafenib by long-term exposure at the respective concentrations of 2 μ M (Rsora 2), 4 μ M (Rsora 4) and 6 μ M (Rsora 6). **C.** Western blot of p-AKT and AKT in unstimulated Huh7 and HepG2 (WT) and in the indicated sorafenib-resistant cell lines. **D.** Western blot of p-AKT in sorafenib-resistant Huh7 and HepG2 cells after incubation to copanlisib for 72 hours. **E. F.** Cell viability assays showing the effect of combined administration of copanlisib and sorafenib in the indicated sorafenib-resistant Huh7 (**E**) or HepG2 (**F**) cells. Error bars represent mean \pm SD of three independent repeats. \neq , $P < 0.05$; O, $P < 0.01$; *, $P < 0.001$.

Figure 6

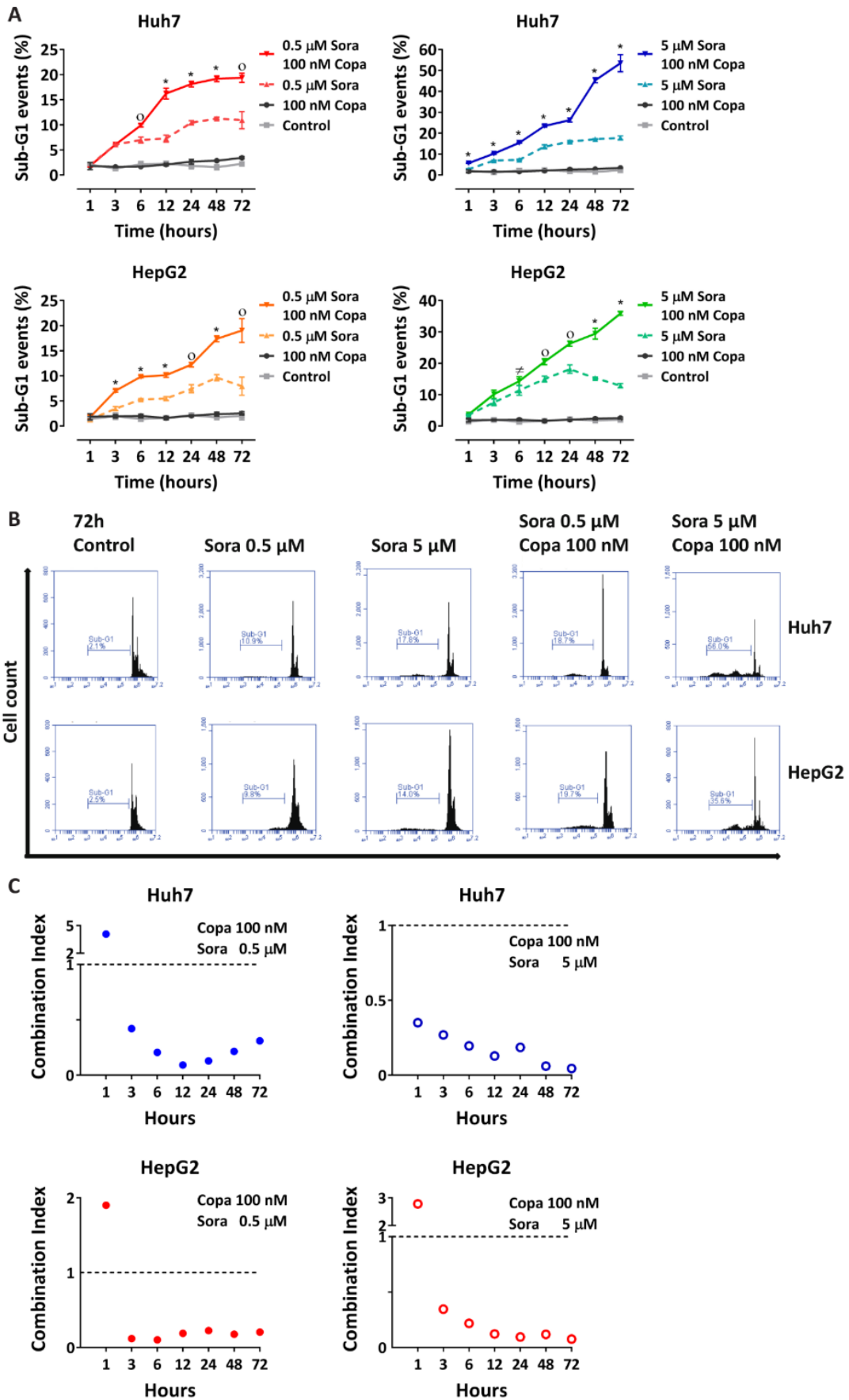


Fig. 6. Copanlisib sensitizes HCC cells to sorafenib by increasing susceptibility to apoptosis. **A.** Sub-G1 events and typical FACS patterns (**B**) after incubation with copanlisib with or without the addition of increasing concentrations of sorafenib in Huh7 and HepG2 cell lines. CI values of <1, 1, and >1 indicated synergistic, additive, and antagonistic effects, respectively. **C.** Combination index (CI) plot of sub-G1 events showing a synergistic interaction of sorafenib and copanlisib in determining apoptosis. Error bars represent mean \pm SD of three independent repeats. \neq , $P < 0.05$; O, $P < 0.01$; *, $P < 0.001$, by independent sample t-test (Copa, copanlisib. Sora, sorafenib).

Figure 7

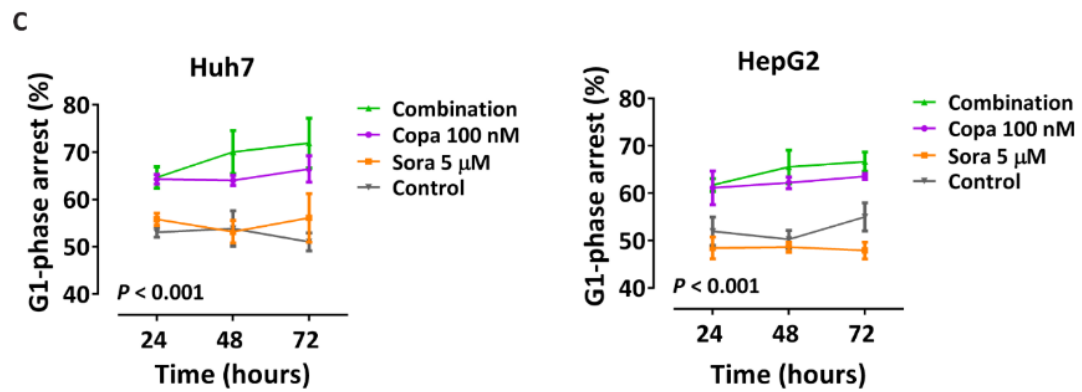
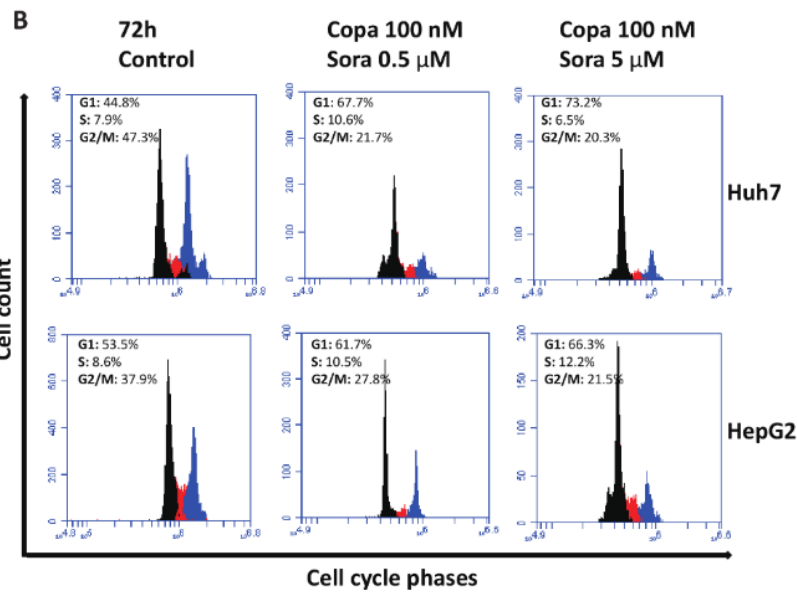
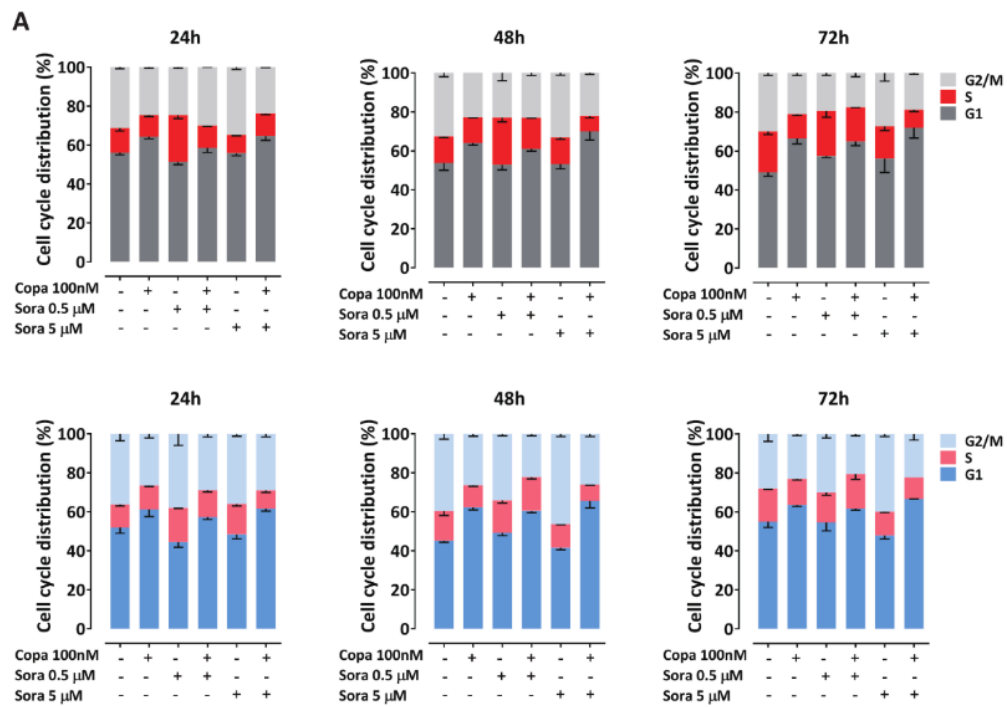


Fig. 7. Copanlisib sensitizes HCC cells to sorafenib by causing cell cycle arrest. A. Cell cycle analysis and typical FACS patterns (**B**) of cells incubated with copanlisib and sorafenib at the indicated concentrations and time points. **C.** Time course of G1-phase. Error bars represent mean \pm SD of three independent repeats. \neq , $P < 0.05$; O, $P < 0.01$; *, $P < 0.001$, by independent sample t-test (Copa, copanlisib. Sora, sorafenib).

Figure 8

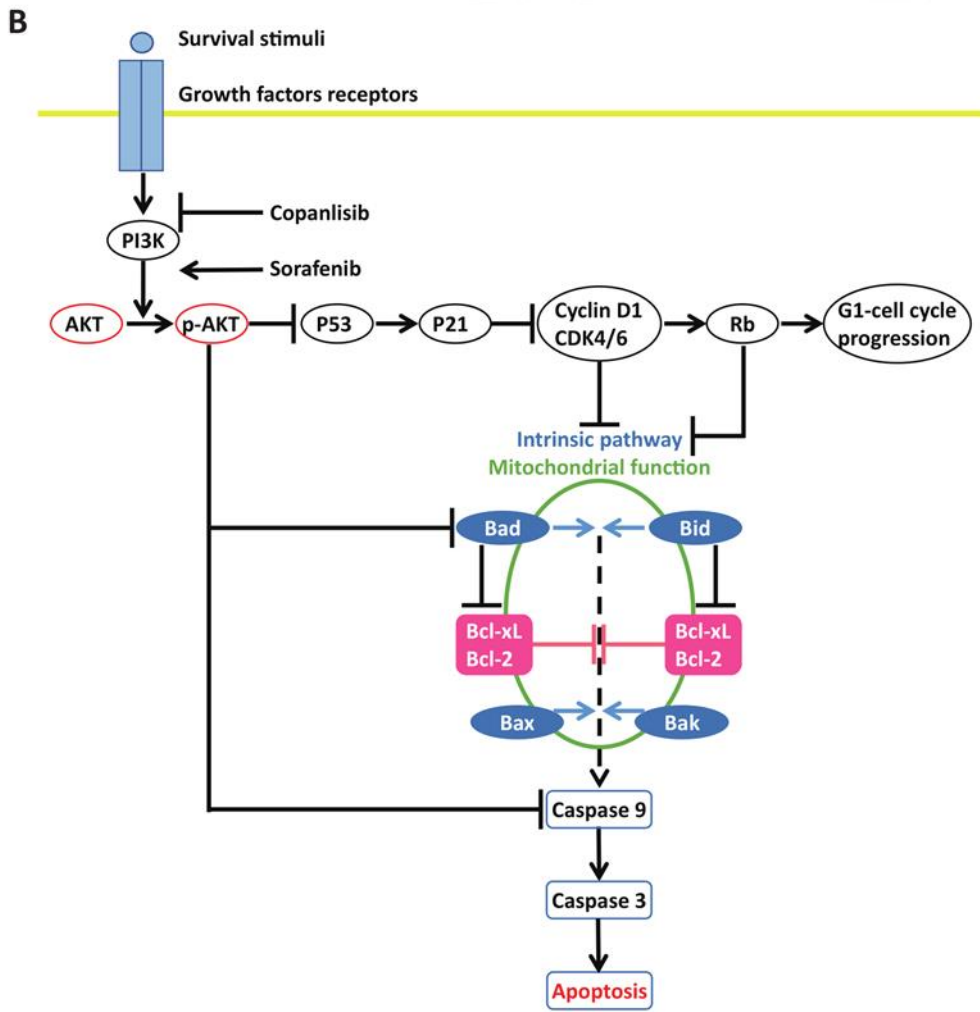
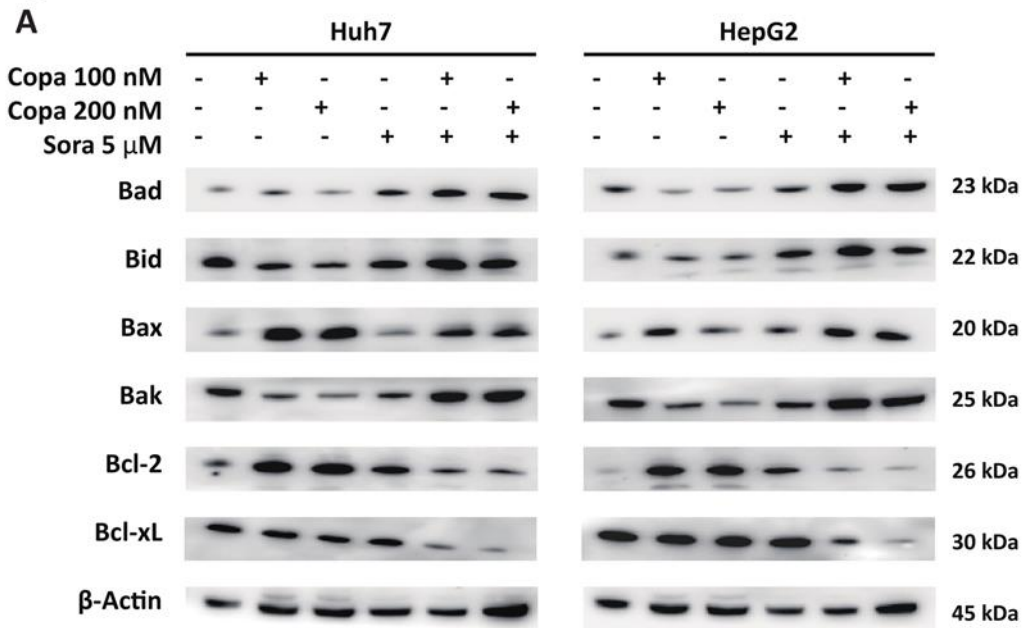


Fig. 8. Effects of copanlisib and sorafenib on different intracellular signaling pathways in HCC cells. **A.** Western blot of critical regulators of apoptosis after stimulation with copanlisib and/or sorafenib for 72 hours. Data are representative of three independent repeats (Copa, copanlisib. Sora, sorafenib). **B.** Schematic diagram describing the hypothesized effect of copanlisib, sorafenib and their interaction on cell cycle and apoptosis.

Prognostic significance and functional relevance of olfactomedin 4 (OLFM4) in the development of hepatocellular carcinoma

ABSTRACT

Background: Olfactomedin 4 (OLFM4) is a secreted glycoprotein predominantly expressed in bone marrow and gastrointestinal tract. Aberrant expression of OLFM4 in human cancers has been reported, but its biological function and significance remain poorly understood in hepatocellular carcinoma (HCC). The purpose of this study is to examine the expression of OLFM4 and its prognostic significance in patients with HCC.

Methods: Immunohistochemical staining to assess expression and cellular distribution of OLFM4 was performed by using a tissue microarray comprising HCC tissues and matched non-tumour tissues from 157 HCC patients. Clinicopathologic characteristics and survival were analysed in 95 patients who underwent partial hepatectomy. The findings were validated *in vitro* by western blot and functional studies using siRNA directed against OLFM4 to assess its effect on cell motility and proliferation.

Results: The fraction of HCC samples exhibiting positive OLFM4 staining in both cytoplasm and membrane was higher in comparison to that observed in hepatocytes from matched non-tumour tissue (61% vs. 39%). Cytoplasmatic staining for OLFM4 was associated with poorer survival ($P = 0.008$), vascular invasion ($P = 0.048$) and MMP-7 expression ($P = 0.002$). Multivariate analysis confirmed that cytoplasmatic staining of OLFM4 was associated with poorer 5-year survival {58.3% vs. 17.3%; HR: 2.135 [95% confidence interval (CI), 1.135 – 4.015]; $P = 0.019$ }.

Conclusion: To our best knowledge, we provide here for the first time evidence on OLFM4 as a marker of prognosis in HCC and identify its role on cell invasion and metastasis formation ².

Prognostische Bedeutung und funktionelle Relevanz von Olfaktomedin 4 (OLFM4) in der Entwicklung des hepatozellulären Karzinoms

ZUSAMMENFASSUNG

Hintergrund: Olfaktomedin 4 (OLFM4) ist ein sekretiertes Glykoprotein, das vorwiegend im Knochenmark und im Gastrointestinaltrakt exprimiert wird. Wohingehend eine anomale Expression von OLFM4 bei humanen Krebserkrankungen bereits berichtet wurde, ist diese beim hepatozellulären Karzinom (HCC) jedoch noch wenig verstanden. Ziel dieser Studie ist es, die Expression von OLFM4 und seine prognostische Bedeutung bei Patienten mit HCC zu untersuchen.

Methoden: Die immunhistochemische Färbung zur Beurteilung der Expression und der Zellverteilung von OLFM4 wurde unter Verwendung eines Gewebemikroarrays durchgeführt, das HCC-Gewebe und passende Nicht-Tumorgewebe von 157 HCC-Patienten umfasst. Die klinisch-pathologischen Merkmale und das Überleben wurden bei 95 Patienten analysiert, die sich einer partiellen Hepatektomie unterzogen hatten. Die Ergebnisse wurden *in vitro* durch Western Blot und Funktionsstudien unter Verwendung von gegen OLFM4 gerichteter siRNA validiert, um dessen Effekte auf die Zellmotilität und -proliferation zu bewerten.

Ergebnisse: Die Fraktion der HCC-Proben, die eine positive OLFM4-Färbung sowohl im Zytoplasma als auch an der Membran zeigten, war höher im Vergleich zu davon Hepatozyten aus übereinstimmendem Nichttumorgewebe (61% vs. 39%). Die zytoplasmatische Färbung von OLFM4 war mit einem schlechteren Überleben ($P = 0,008$), einer Gefäßinvasion ($P = 0,048$) und der MMP-7-Expression ($P = 0,002$) verbunden. Eine multivariate Analyse bestätigte, dass die zytoplasmatische Färbung von OLFM4 mit einem

schlechteren 5-Jahres-Überleben verbunden war (58,3% vs. 17,3%; HR: 2,135 [95% -Konfidenzintervall (CI), 1,135 - 4,015]; $P = 0,019$).

Schlussfolgerung: Nach unserem besten Wissen konnten wir hier erstmals OLFM4 als einen Marker für die Prognose des HCCs nachweisen und seine Rolle für die Zellinvasion und Metastasierungsbildung aufzeigen.

INTRODUCTON

Hepatocellular carcinoma (HCC) is one of the leading causes of cancer-related death worldwide with approximately 800,000 people dying each year ^{5,39}. In very early disease stages HCC can be treated in curative intention via surgery or local ablative procedures. Unfortunately, most patients are diagnosed in advanced stages or progress under therapy to stages ⁴⁰. The identification of new markers that are functionally involved in tumour development and progression may contribute to identify patients who are at high risk of tumour progression and could benefit from more intensive treatment or surveillance under therapy.

Olfactomedin 4 (OLFM4, also known as GW112 or hGC-1), is a secreted glycoprotein found in different tissues, comprising hematopoietic myeloid cells, the gastrointestinal tract, and prostate ⁴¹. Overexpression of OLFM4 has been found in solid neoplasm such as gastric ⁴², colorectal ⁴³, pancreatic ⁴⁴, lung, and breast cancer ⁴⁵ as well as in leukemia cells ⁴⁶. Furthermore, an association of OLFM4 and liver metastases of colorectal cancer was described earlier ⁴⁷. Increased OLFM4 mRNA levels has been shown in gastric, colon, pancreatic, breast and lung cancers at initial stages ^{45,48,49}; in addition, serum OLFM4 levels were significantly higher in patients with gastric cancer than in non-tumor patients ⁵⁰. It has thus been suggested that OLFM4 is a marker of gastrointestinal cancer development and that its expression could be used as biomarker to identify patients who are at greater risk for disease progression ^{51,52}. Specifically, functional studies have shown that OLFM4 might play a role in determining cell motility and metastasis formation, since high expression levels of OLFM4 have been found to decrease adhesion and increase migration in colon cancer cells ⁵². OLFM4 was also shown to attenuate apoptosis via inhibiting the intrinsic apoptotic pathway by a blockade of caspase 3 and caspase 9 in gastric and prostate cancer cells ^{53,54}. Genetic alterations of OLFM4 have been found to

correlate with tumour differentiation, metastasis formation and prognosis in numerous cancers, suggesting that OLFM4 could be used as an early marker of tumor development ⁵⁵.

In summary, although cumulative evidence points to a role of OLFM4 in cancer development, the relevance of this molecule in the pathogenesis of HCC has not yet been investigated. To address this issue we thus examined the expression and cellular distribution of OLFM4 in HCC tissues and matched non-tumour tissues, and investigated the potential relationship of OLFM4 staining with patient clinicopathologic features and survival.

MATERIALS AND METHODS

Patients and pathologic material

Patients with HCC who underwent liver transplantation or partial liver resection at the University Hospital, LMU Munich during the time-period 1985 and 2015 were considered for the study. To avoid a potential bias related to the exceptionally favourable prognosis of patients undergoing liver transplantation, patients who received liver transplantations were not considered for analysis of survival. Data on survival were obtained from the Munich Cancer Registry (MCR; <http://www.tumorregister-muenchen.de>). Archival pathological material from the Institute of Pathology of the University of Munich. The characteristics of the tissue microarray containing tumour samples and matched tumor tissues has been previously described ⁵⁶.

Immunohistochemical staining

Sections (5 µm) of tissue microarray blocks were used for immunohistochemical staining. Anti-OLFM4 polyclonal rabbit antibody (BIOZOL GmbH, Germany), anti-MMP-7 monoclonal mouse antibody (Merck KgaA, Germany), and anti-E-cadherin monoclonal mouse antibody (Cell Signaling Technology, USA) were applied as primary antibodies. Samples have been processed for antigen retrieval as previously described ⁵⁷. Vectastain ABC Elite Universal (Vector Laboratories Inc., USA) kit was used for immunohistochemical staining; AEC (Zytomed Systems, Germany) was used as a chromogen. Positive staining for OLFM4 was categorized according to its cellular distribution and independently of total staining intensity according to the following categories: cytoplasmic staining; staining on cell membranes only; positive staining signals in both cytoplasm and cell membrane. In addition, we conducted a semiquantitative analyses by categorizing samples according to the percentage of cells exhibiting staining for

OLFM4 as follows: score 0: no staining; score 1: staining in < 30% of cells; 2: staining in 30% to 70% of cells; 3: staining in > 70% cells. Concerning OLFM4 cytoplasmic staining: score 0, negative staining; score 1, weak staining; score 2, strong staining.

Histologic assessment of tumours and surrounding non-tumour tissues

Tumor grading according to the WHO criteria ⁵⁸, presence of vascular invasion, number and size of tumor lesions (as defined by macroscopic inspection of surgical specimens) were analysed as tumor-associated pathological variables. Matched tissues not containing tumor material were analysed features related to the underlying liver disease and comprised the presence and quantification of fibrosis/cirrhosis, of portal inflammation, piecemeal necrosis, and steatosis. Histologic evaluation performed on haematoxylin and eosin-stained slides and evaluated by a senior pathologist and two of the authors who had not prior knowledge of prognostic data. The Ishak score was used to evaluate liver fibrosis, portal inflammation, and piecemeal necrosis ⁵⁹. The nonalcoholic fatty liver disease activity score and staging system was used for assessment of steatosis and lobular infiltration ⁶⁰.

Cell culture

Huh7 and PLCPRF5 cells (ATCC, USA) were cultured in Dulbecco's Modified Eagle's Medium (DMEM; Sigma Aldrich, Germany) with 10% Fetal Bovine Serum (FBS; Biochrom GmbH, Germany) and 1% Penicillin-Streptomycin (Sigma Aldrich, Germany). Cells were maintained in 5% CO₂ at 37°C. Authentication of cell lines was conducted by Leibniz Institute DSMZ-German Collection of Microorganisms and Cell Cultures.

Human tissue for isolation of primary human hepatocytes

Double-coded tissues and corresponding data used in this study were provided by the Biobank of the Department of General, Visceral and Transplantation Surgery, Ludwig Maximilian University (LMU), Munich, Germany, under the administration of the Human Tissue and Cell Research (HTCR) Foundation. The framework of HTCR Foundation ⁶¹, which includes obtaining written informed consent from all donors, has been approved by the ethics commission of the Faculty of Medicine at the LMU (approval number 025-12) as well as the Bavarian State Medical Association (approval number 11142), Germany. Primary human hepatocytes were isolated by the Cell Isolation Core Facility of the Biobank using a two-step collagenase perfusion technique with modifications, as described earlier ⁶².

Western blot

Equal amount of proteins in each sample was loaded on 10% or 12% SDS-PAGE gels and separated for 25 minutes at 80 V and for 80 minutes at 120 V, then transferred onto PVDF membranes (EMD Millipore Corporation, USA). After blocking for 1 hour in TBST (Tris-Buffered Saline with Tween-20) containing 5% milk or 5% bovine serum albumin (Carl Roth, Germany), membranes were incubated overnight at 4°C with the following primary antibodies: OLFM4, MMP-2 (Cell Signaling Technology, USA), MMP-7, MMP-9 (Cell Signaling Technology, USA), E-cadherin, and β -actin (Cell Signaling Technology, USA). Subsequently the membranes were probed with horseradish-peroxidase conjugated secondary anti-rabbit or -mouse IgG antibodies (GE Healthcare, UK Limited) for 2 hours at room temperature at the dilution of 1:10,000. The bands were visualized by SuperSignal West Pico Chemiluminescent Substrate (Thermo Scientific, Germany) and photographed with an image acquisition system, ECL ChemoCam Imager (Intas GmbH, Germany).

siRNA interference

Cells were plated to reach a confluence of 40% to 60%. After overnight incubation, cells were transfected using Oligofectamine (Invitrogen, Germany) and siRNA directed against OLFM4 (siRNA-1, sense: GAGUUAACCUGACCACCAATT, antisense: UUGGUGGUCAGGUUAACUCTG. siRNA-2, sense: GGGAUUCUUUGUACAGGAATT, antisense: UUCCUGUACAAAGAAUCCCTA. Qiagen, Germany) or with beta-galactosidase (Dharmacon Inc., USA), which served as control at a final concentration of 50 nM. Serum-containing medium was added 4 hours after transfection. Silencing of OLFM4 was confirmed by immunoblotting 24 hours after transfection.

Immunofluorescence

75,000 cells/well were plated on round cover slips (Thermo Scientific, Germany) with a diameter of 18 mm in 6-well plates (NUNC, Germany). After 24 hours after transfection with siRNA cells were fixed in paraformaldehyde (4%, Carl Roth, Germany) for 15 minutes, treated with 0.15% Triton X-100 (Sigma-Aldrich, Germany) for 15 minutes in PBS (Invitrogen, Germany), then blocked for 30 minutes with 5% BSA in PBS. Samples were incubated with antibodies against OLFM4 and E-cadherin diluted in blocking solution at 1:200 at 4°C overnight and after washing, subsequently incubated for 1 hour with goat anti-rabbit antibody conjugated with Alexa Fluor 488 (Invitrogen, Germany) at 1:200 dilution. After three washes with PBS, slides were mounted with Vectashield (Vector Laboratories Inc., USA) containing Hoechst 33342 (Sigma-Aldrich, Germany). Pictures were taken using the Axiovert 135 TV fluorescence microscope (Zeiss, Germany).

Flow cytometry

Sub-G1 events and cell cycle distribution were assessed to measure apoptosis and different phases of cell cycle by using fluorescence-activated cell sorter (FACS), Accuri C6 Flow Cytometer and BD Accuri C6 software (BD Biosciences, Germany). Cells were seeded in 6-well plates to reach a confluence of 50% to 60% before undergoing transfection with siRNA. After 24 hours, the cells were split by trypsin (Invitrogen, Germany), collected and washed with sterilized, ice-cold PBS once, then incubated in staining buffer containing 0.1% sodium citrate (Carl Roth, Germany), 0.1% Triton X-100 and 50 µg/ml propidium iodide (PI; Sigma-Aldrich, Germany).

Proliferation assay

1,000 to 1,500 cells were seeded in 96-well plates (NUNC, Germany) cultured overnight and then incubated with siRNA. After 6 days, cells were washed with PBS and underwent osmotic lysis in 100 µl ddH₂O for 45 minutes at 37°C. 0.2% Sybr green (Lonza, USA) was added to each well, fluorescence was measured and proliferation index was calculated as a ratio to untreated samples. Three independent experiments were performed per agent, with each data point reflecting triplicate wells. Error bars represent standard deviation (SD) of the mean from three experiments.

Scratch assay

Cells were seeded in 6-well plates to reach a confluence of 80% and treated as indicated in the siRNA section. After cells became confluent, a scratch was made through by a sterile micropipette tip (Sarstedt AG & Co., Germany). The scratch-area was photographed after the scratch was performed and after 24 hours to assess cell migration within the wounded area. Migration was quantified by measuring the area of the scratched regions by ImageJ software

(National Institutes of Health, Bethesda, Maryland, USA, <https://imagej.nih.gov/ij/>). The experiment was performed three times.

Migration and invasion assay

The chamber of 8- μm transwell inserts (Corning, USA) with or without Matrigel (Corning, USA) was used for migration and invasion assay. 2×10^5 cells underwent incubation in the serum-free top chamber while serum-containing medium was added to the lower chamber. To assess the fraction of cells which migrated, staining with 1% crystal violet (Sigma-Aldrich, Germany) was performed after 24 hours of incubation and fixation in 10% formalin (Carl Roth, Germany). For microscopy cells were evaluated at a magnification of $\times 200$ (Zeiss, Germany).

Cancer genome atlas analyses

Publically available RNA sequencing data of HCC samples ($N = 423$) were downloaded from The Cancer Genome Atlas (TCGA) (<http://cancergenome.nih.gov/>). The analyses of fragments per kilobase of transcript per million fragments (FPKM) values of genes in TCGA HCC patient samples and survival outcome were conducted as previously described ⁶³.

Statistical analysis

All statistical analyses were calculated using SPSS (version 24; SPSS, Inc.). For frequency data, exact χ^2 tests were used. Differences between groups were calculated by the Student's *t*-test. Overall survival was estimated with the Kaplan-Meier method and tested with the log-rank procedure. For analysis of survival a Cox proportional hazards regression model was used and reported by hazard ratios (HR) and 95% confidence intervals (CI). Statistical significance was set for a *P* value < 0.05 .

RESULTS

Patients and clinicopathological parameters.

157 HCC patients included in the constructed TMA from surgical specimens of patients undergoing liver resection or liver transplantation were considered for clinicopathological analysis. To avoid biases related to the effect of transplantation on patients' outcome, 56 patients who had undergone liver transplantation were not considered for survival analysis, which was performed in 95 out of 101 patients with available survival data. The demographic and clinicopathologic characteristics of the patients in our cohort are presented in **Table 1**. For patients included in the survival analysis, the median follow-up time was 22 months. The median follow-up for survivors was 42 months vs. 17 months for deceased patients.

Immunohistochemical staining for OLFM4 in HCC cells and in hepatocytes from surrounding non-tumour tissues.

In non-tumour tissues, OLFM4 stained positive in altogether 68.5% showing a pattern of mixed membrane and cytoplasmatic staining in 39.5% of patients, of cytoplasmatic staining only in 27.3% of patients, and a membrane-only staining in 1.7% of samples. No staining for OLFM4 could be detected in 31.5% of samples from non-tumor tissues. In HCC samples, altogether 87.6% showed a positive staining for OLFM4: cytoplasmatic staining for OLFM4 (26% of samples) was similar to that observed in non-tumor tissues, whilst the fraction of patients with staining on both membranes and cytoplasm increased to 61.6% (**Fig. 1A, B**). Altogether, OLFM4 staining in cell cytoplasm was more common than in matched, surrounding HCC lesions (OLFM4: 66.8% in normal cells versus 87.6% in HCC; Pearson's χ^2 test: $P < 0.001$). This difference was

principally due to the higher fraction of HCC samples showing a pattern of mixed cytoplasmatic and membrane staining for OLFM4 (61.6% of tumor samples versus 41.2% of nontumor samples exhibited positive membrane staining for OLFM4; Pearson's χ^2 test: $P < 0.001$).

Correlations between OLFM4 staining and clinical and pathological characteristics of tumour tissues and non-tumour tissue samples.

We next assessed the correlation between OLFM4 staining in both tumour and non-tumor specimens and the available demographic and clinicopathologic features of the collective, including etiology of underlying liver disease, age and gender of patients, presence of liver cirrhosis, grading and size of tumors and the presence of vascular invasion. In addition, established immunohistochemical markers related to cell invasion and aggressive phenotype in HCC, including expression of E-cadherin⁶⁴ and MMP-7 were included in the analysis (**Table 2**).

Positive cytoplasmatic staining for OLFM4 in tumour samples was associated to the presence of lobular inflammation in the surrounding non-tumour tissue ($P < 0.001$), MMP-7 expression ($P = 0.002$) and blood vessel invasion ($P = 0.048$). Furthermore, significant association was observed between the membrane staining for OLFM4 and the expression of E-cadherin ($P = 0.042$) and MMP-7 ($P = 0.015$) in tumor samples. In contrast, no relevant correlation were found between clinicopathologic variables and OLFM4 staining in matched non-tumour tissues samples (data not shown).

Prognostic significance of OLFM4 staining in patients undergoing liver resection.

Since the higher prevalence of OLFM4 staining in tumor samples suggested a role of this molecule in tumor development, a survival analysis was performed to assess the prognostic significance of OLFM4 in patients undergoing partial hepatectomy (**Fig. 2A**). A Kaplan-Meier analysis revealed the presence of vascular invasion (**Fig. 2B**; $P = 0.002$) and cytoplasmatic staining of OLFM4 (**Fig. 2C**; $P = 0.008$) as predictors of survival. Specifically, patients showing OLFM4 staining in the cell cytoplasm had a poorer outcome compared to patients without cytoplasmatic staining for OLFM4 (5-year overall survival: 58.3% versus 17.3%, respectively). This was corroborated by a survival analysis performed according to semiquantitative criteria defining OLFM4 cytoplasm staining intensity (negative, weak and strong - **Fig. 2D**; 5-years overall survival were 70.7%, 21.6%, and 15.7%, respectively, $P = 0.005$). In contrast, membrane staining did not affect survival (**Fig. 2E**; $P = 0.154$, **Fig. 2F**; $P = 0.123$). In addition, survival analyses based on presence or absence of OLFM4 staining, regardless of cellular distribution or intensity, was not associated with patients' outcome, suggesting that in addition to higher expression, cellular distribution plays a role in determining the functional effect of OLFM4 during tumor development (**Fig. 2G**, $P = 0.147$; **2H**, $P = 0.166$). This was confirmed by assessment of mRNA expression in an independent cohort of HCC patients obtained from the publically available database of the TCGA showing that, survival of patients exhibiting high OLFM4 expression was numerically higher, but not statistically different, than in patients with low mRNA expression (**Fig. 3A**, $P = 0.0604$).

In addition, mRNA expression analysis confirmed the correlation observed at immunohistochemical level between OLFM4 expression and E-cadherin (**Fig. 3B**, $r = -0.102$, $P = 0.036$) and MMP-7 (**Fig. 3C**, $r = 0.456$, $P < 0.0001$) in TCGA HCC cohorts, thus corroborating the finding that OLFM4 might

contribute to worse prognosis by impinging on these two regulator of cell motility and invasion.

Cox univariate analyses taking into account age, gender, etiology, the existence of cirrhosis and steatosis, liver inflammation, necrosis, grading, tumor size, the presence of metastasis and multifocal lesions, the expression of E-cadherin and MMP-7, or signs of blood vessel invasion showed that the cytoplasm staining of OLFM4 (HR: 2.226; 95% CI: 1.186 – 4.177; $P = 0.013$) and vessel invasion (HR: 1.879; 95% CI: 1.181 – 2.989; $P = 0.008$) independently influence the survival of HCC patients after partial hepatectomy (**Table 3**). Cox multivariate analyses calculated HRs for OLFM4 cytoplasm staining was 2.135 (95% CI: 1.135 – 4.015; $P = 0.019$) and for vessel invasion was 1.791 (95% CI: 1.124 – 2.854; $P = 0.014$; **Table 4**). In contrast, no correlation was found between OLFM4 staining in non-tumour surrounding tissues and survival of patients (data not shown).

OLFM4 silencing suppresses cell migration and invasion, and causes cell cycle arrest *in vitro*.

To assess the functional relevance of OLFM4, and validate *in vitro* the observed association between this protein and MMP-7, or E-cadherin observed in immunohistochemical studies, we assessed the effect of silencing of OLFM4 by siRNA and its basal expression in HCC cancer cells and in primary human hepatocytes (**Fig. 4A, C**). As shown in **Fig. 4B**, the effect of siRNA-silencing on OLFM4 was observable within 24 hours. As expected, OLFM4 knockdown inhibited the expression of MMP-7, -2, and -9, and increased the expression of E-cadherin levels. Consistently, both cytoplasm and membrane expression of OLFM4 were diminished after siRNA-silencing incubation as shown by

immunofluorescence in HCC cell lines (**Fig. 4D**). As alterations of E-cadherin and MMP-family molecules are involved in the process of cell invasion and the development of metastasis ⁶⁵⁻⁶⁷, we performed scratch- and transwell-assays to determine the effect of OLFM4 silencing on cell invasion and metastasis *in vitro*. To this regard, we observed that cell motility was greatly diminished in OLFM4-siRNA transfected cells vs. control cells as judged both by the assessment of healing areas at the scratch assay (**Fig. 5A-C**) and by decreased cell migration in transwell chambers (**Fig. 5D-H**). These results indicate that OLFM4 impinges on cell motility and invasive properties and represent a correlate for the immunohistochemical and prognostic data.

Finally, as OLFM4 was previously reported to affect apoptosis ^{68,69}, we here investigated whether OLFM4, besides affecting cell motility, also affects cell viability and proliferation. As shown by the significant increase of sub-G1 events after PI-staining, we found a small but significant increase of apoptosis after siRNA-OLFM4 incubation for 24 hours (**Fig. 5I, J**). In addition, a G1 cell cycle arrests was observed, along with a corresponding decrease of the S and G2/M phases of cell cycle (**Fig. 5I, J**).

Taken together, these results indicate that OLFM4 down-regulation affects the viability of HCC cells mainly by activating apoptosis and inducing G1 cycle arrest. The corresponding expressive variation of MMP family and E-cadherin reveals the important role of OLFM4 in HCC adhesion and metastasis.

DISCUSSION

Staining, localization and prognostic significance of OLFM4 in tumours versus surrounding non-tumour tissues.

OLFM4, also known as GW112 or G-CSF-stimulated clone 1 protein (hGC-1), is a glycoprotein with a molecular weight of 64 kDa originally cloned from human myeloblasts⁷⁰. OLFM4 is known to play multiple roles as a mediator of inflammation and cellular differentiation^{41,71}. However, evidence has accumulated on the fact that OLFM4 plays a role in the development of different tumor entities and might contribute to determine chemoresistance^{50,52,72}. To the best of our knowledge, no systematic study has been conducted to assess the prognostic relevance of the OLFM4 family in HCC.

In agreement with the notion that OLFM4 expression plays a role in cancer formation, we found that 87.6% of cancer samples, but only 68.5% of matched non-tumour samples exhibited a positive staining of OLFM4 (**Fig. 1**). This is in accordance with previous findings showing that OLFM4 was significantly higher in serum of patients with solid tumours such as gastric, colorectal, pancreatic, head and neck, or prostate cancers than in healthy individuals⁵⁵.

Interestingly, however, as we assessed the prognostic significance of OLFM4, no association between survival and overall staining or semiquantitative staining intensity of OLFM4 at immunohistochemistry or by stratifying patients by mRNA expression levels could be found. As we categorized our samples according to the fraction of tumours exhibiting OLFM4 staining on cell membrane vs. samples with cytoplasmatic staining, we observed that tumor and non-tumor samples essentially differed in the proportion of specimens with a cytoplasmatic staining (**Fig. 1**). Correspondingly, as we assessed the relevance of OLFM4-expression on survival in HCC patients, five-year survival of

patients with tumours exhibiting OLFM4 staining in cell cytoplasm showed a poorer prognosis in comparison to patients without OLFM4 staining (**Fig. 2C, E; Table 3, 4**).

Previous immunohistochemical studies have reported that OLFM4 can be localized in virtually all cell compartments including the mitochondria^{46,54}, and the cell nucleus⁵⁴. In addition, OLFM4 is known to be secreted⁷³ outside the cell and to be detectable in plasma of patients. The cytoplasmatic localization observed in our samples likely represents the functional correlate of OLFM4 with histological type and differentiation of HCC.

Clinical-pathologic correlations of OLFM4 staining and functional assessment of OLFM4 *in vitro*.

To assess the role of OLFM4 in the pathogenesis of HCC, we attempted at finding a correlation between OLFM4 staining and pathological features defining the severity of the liver disease underlying the occurrence of HCC in the patients of our collective, and hypothesized that increasing severity of liver disease (e.g. increasing fibrosis, steatosis or lymphocyte infiltration) would be accompanied by increasing staining of OLFM4. To this regard, we observed that cytoplasm staining for OLFM4 in tumour samples was associated with lobular inflammation of liver ($P < 0.001$), which possibly reflects an unfavorable effect of OLFM4 on tumor inflammation (**Table 2**)⁷⁴. Furthermore, as we assessed the correlation between OLFM4 and tumor-specific clinical-pathological characteristics, we found a correlation between staining for OLFM4 and blood vessel invasion ($P = 0.048$), staining for MMP-7 ($P = 0.002$) and of E-cadherin status ($P = 0.042$; **Table 2**). This was confirmed by the analysis of the correlation between OLFM4, E-cadherin and MMP-7 mRNA expression

observed in the second independent cohort, and by *in vitro* experiments, which confirmed the causal relationship between expression of OLFM4 and that of E-cadherin and MMP-7. In addition, these *in vitro* experiments confirmed the functional role of OLFM-4 in determining cell viability and metastatic properties of cancer cells. Collectively, our findings show that OLFM4 may play a role in regulating tumour invasiveness in HCC cells by activating MMP-7 expression, which causes degrading of the basal membrane and inhibits E-cadherin expression (**Fig. 6**), thus contributing to the malignant phenotype of HCC.

Possible clinical consequences of OLFM4 expression in liver cancer cells.

Although the mechanism, by which OLFM4 overexpression causes the reported bad prognostic effects in tumour cells, our results are in keep with that of several other studies which provided evidence that increased OLFM4 expression is associated with an aggressive tumor phenotype^{42-45,47}. The multivariate analysis of our data, comprising the determination of tumor stage at diagnosis and other important characteristics like vascular invasion, define OLFM4 as a prognostic marker for HCC, suggesting that OLFM4 could be investigated prospectively as marker of aggressiveness and, as previously suggested^{41,55}, as a marker of response to treatment. To this regard, future studies will have to address the issue of the role played by OLFM4 within well-established, potentially actionable signalling pathways, such as the PI3K-Akt-Tor signalling, beta-catenin, RAS-RAF-MEK-ERK, PDGF, and MET signalling. In addition, serum OLFM4 levels have been proposed as a biomarker for gastric and colorectal cancer with the potential of identifying patients at risk of recurrence or progression^{50,52,75}. Whether this could be translated to the case of HCC – thus

providing a circulating marker of aggressiveness and possibly of response to treatment, will be the interesting object of future studies.

Summary

Increased expression of OLFM4 is a common event in the pathogenesis of HCC. These findings warrant further investigation of the role of this molecule in mediating development of HCC and in particular its role in determining the metastatic properties of cancer cells.

FIGURES

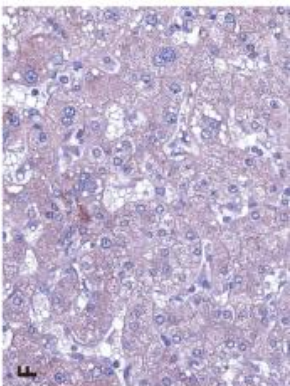
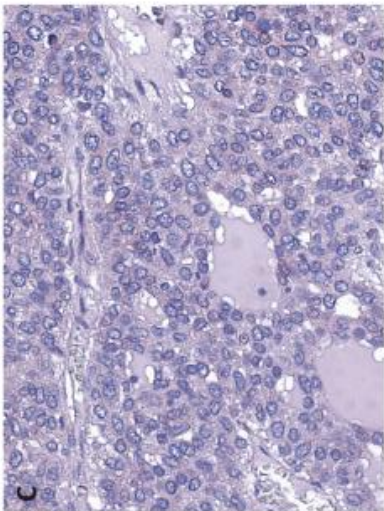
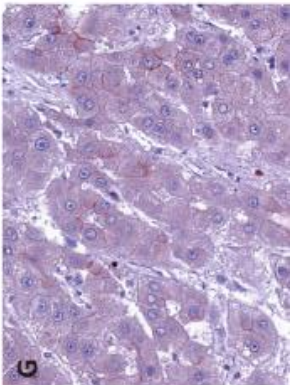
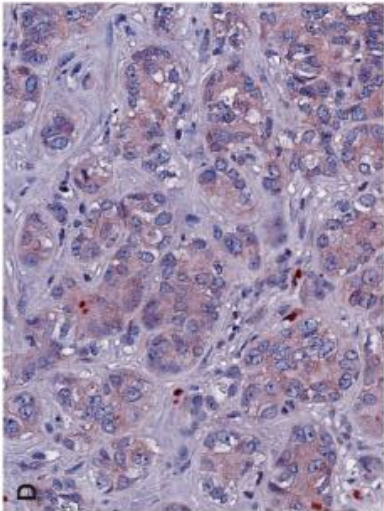
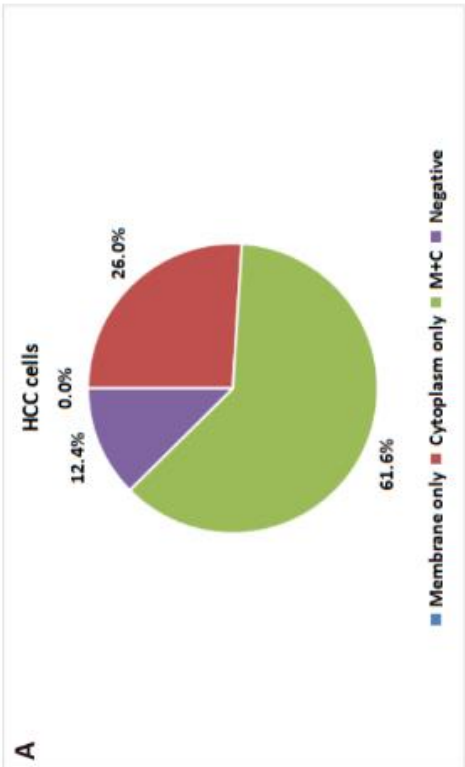
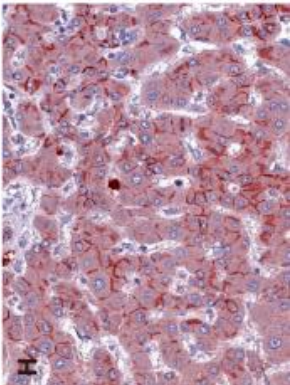
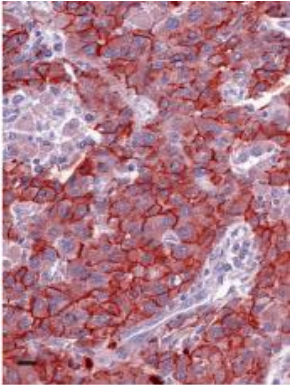
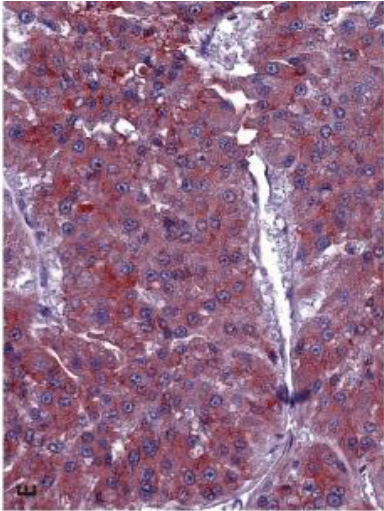
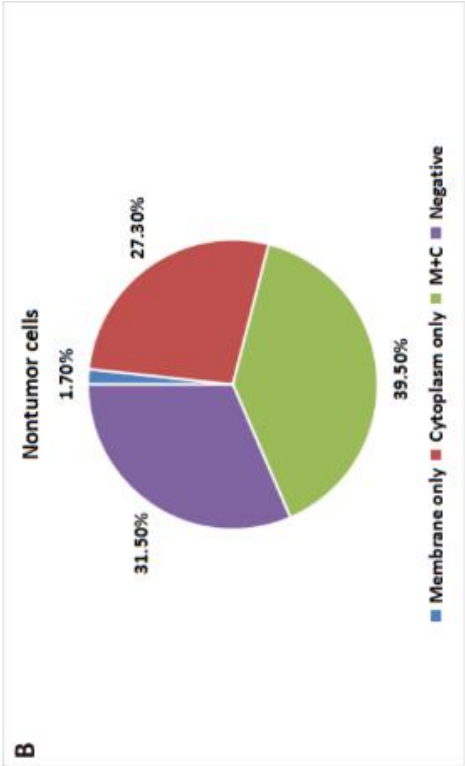


Fig. 1. Expression and cellular distribution of OLFM4 in tumor and non-tumor tissue samples. **A. B.** Staining of OLFM4 in HCC cells and in non-tumor cells: proportion of samples showing no staining (none), cytoplasmatic staining (cytoplasm only), membrane staining (membrane only), or both (m+c). Representative cytoplasm staining pattern in HCC samples: **(C)** score 0, negative; **(D)** score 1, weak; **(E)** score 2, strong. Representative typical positive membrane and cytoplasm staining in HCC tissues: **(F)** score 0, negative; **(G)** score 1, less than 30% of cells; **(H)** 30% - 70% of cells; **(I)** over 70% of cells. Magnification, x 40.

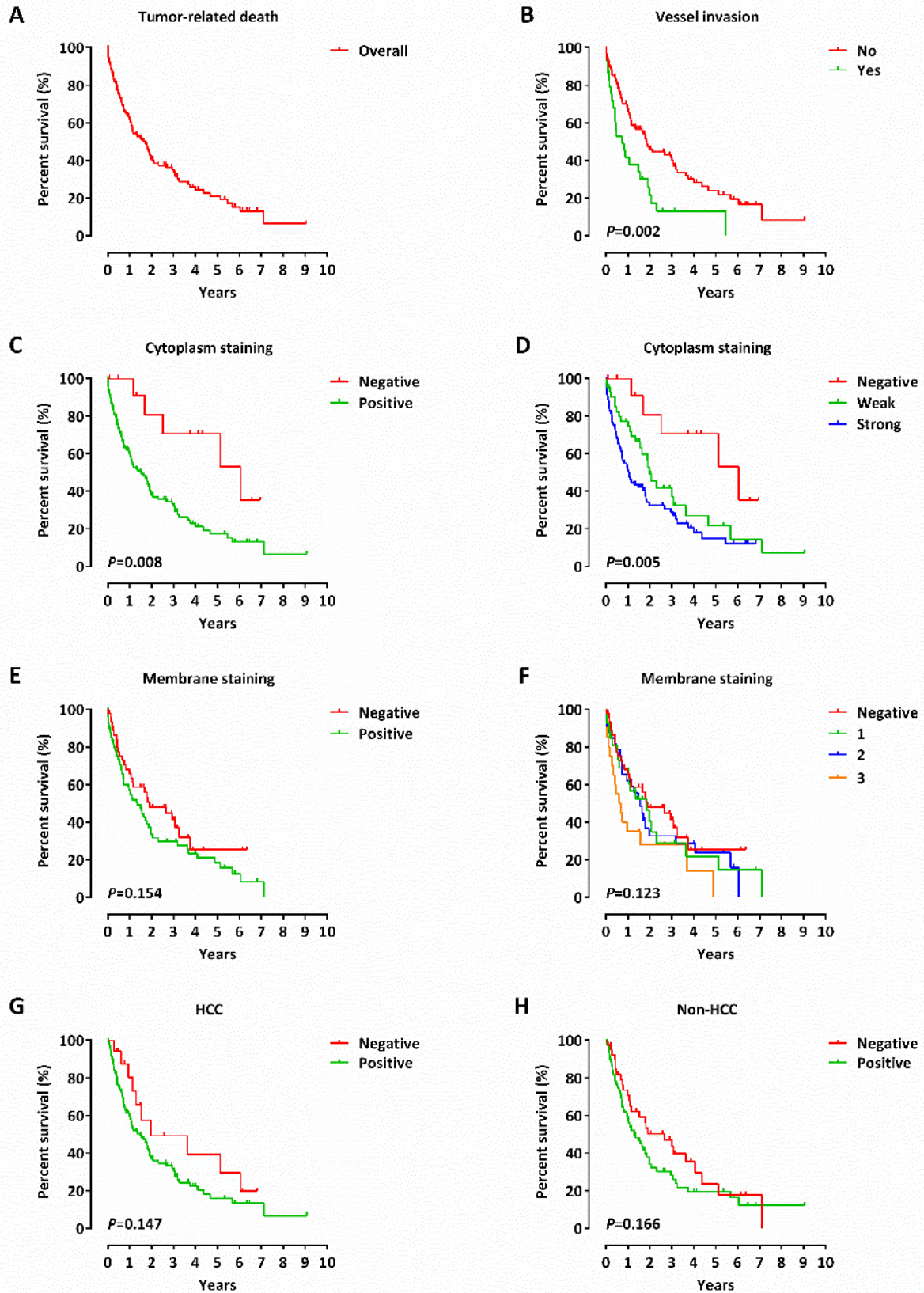


Fig. 2. Prognostic significance of OLFM4 according to cellular distribution. **A.** Overall survival (OS) of the entire patients' collective as determined by the Kaplan-Meier method. **B.** OS according to evidence of vessel invasion. OS according to cytoplasm staining for OLFM4 (positive or negative (**C**)) or according to semiquantitative assessment of staining intensity (**D**). OS according to membrane staining for OLFM4 (positive or negative (**E**)) or according to semiquantitative assessment of staining intensity (**F**). **G.** Overall survival (OS) according to OLFM4 staining in HCC tissues and in non-HCC tissue samples (**H**). +: Censored cases.

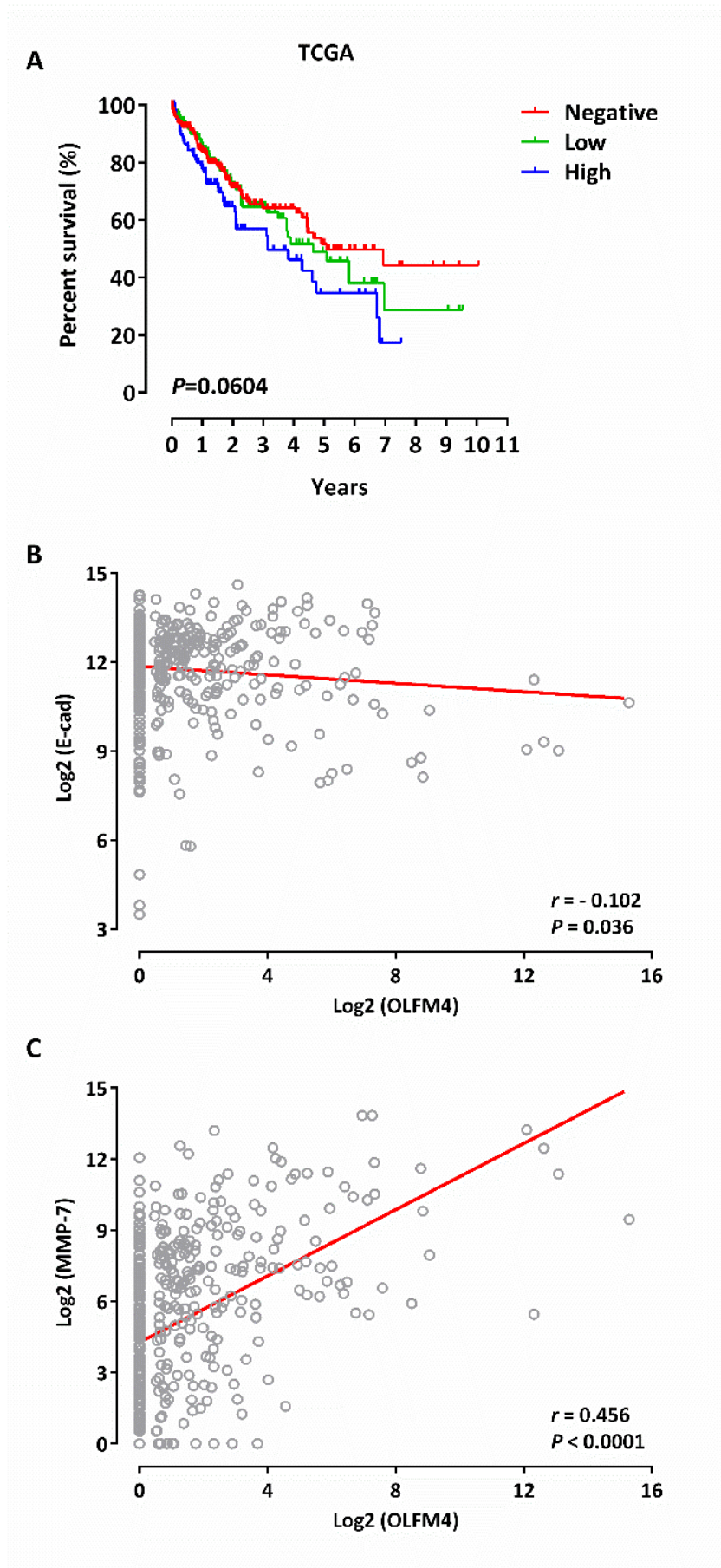


Fig. 3. Prognostic significance of OLFM4 and correlation with E-Cadherin or MMP-7 according to mRNA expression analysis of an independent cohort. A-C, expression of OLFM4 mRNA in a second independent cohort of HCC patients. (A) Kaplan-Meier survival curves according to mRNA expression levels. Assessment of the correlations between OLFM4 and E-cadherin (B) or MMP-7 (C) mRNA expression levels from the same patients' collective.

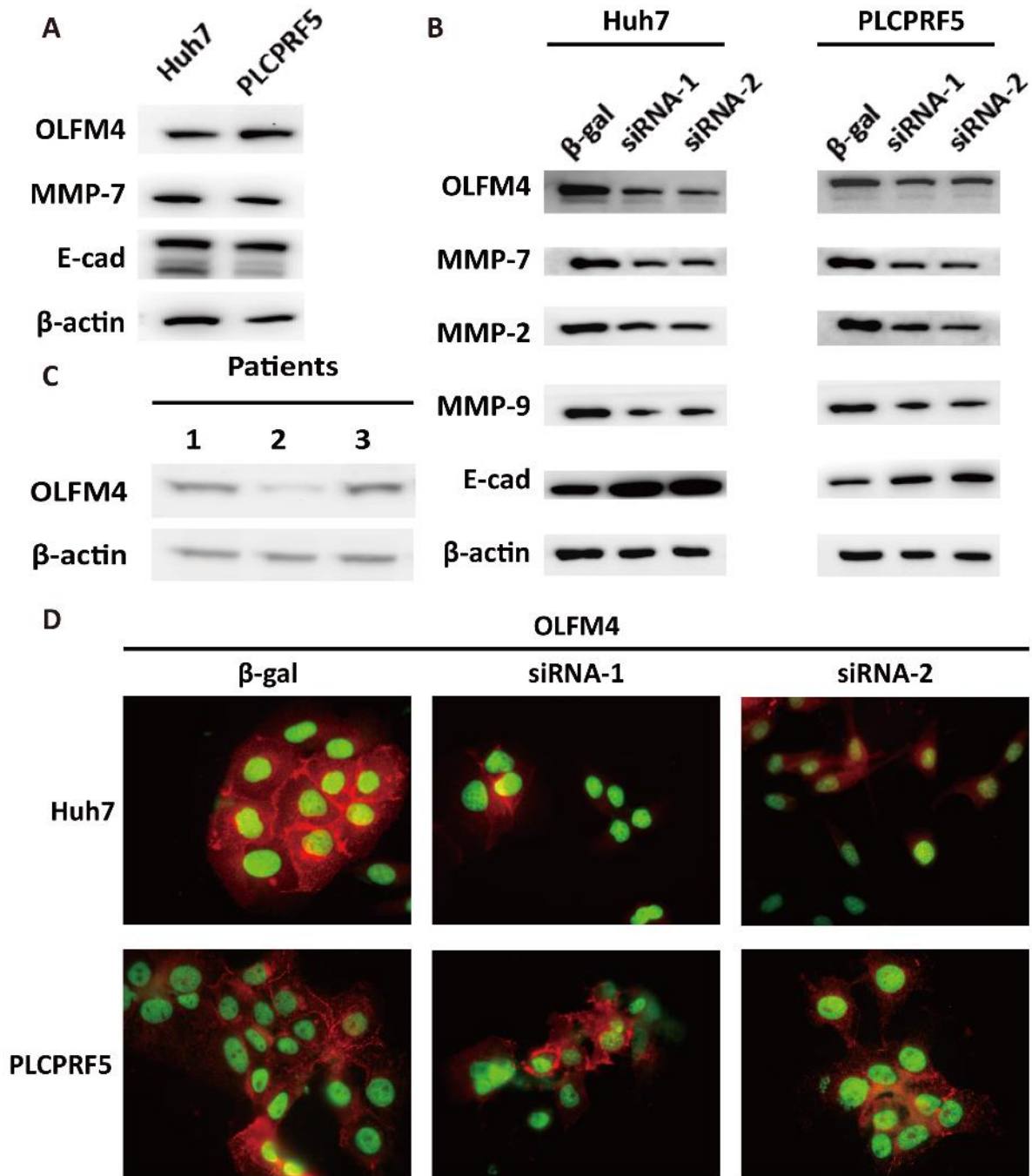
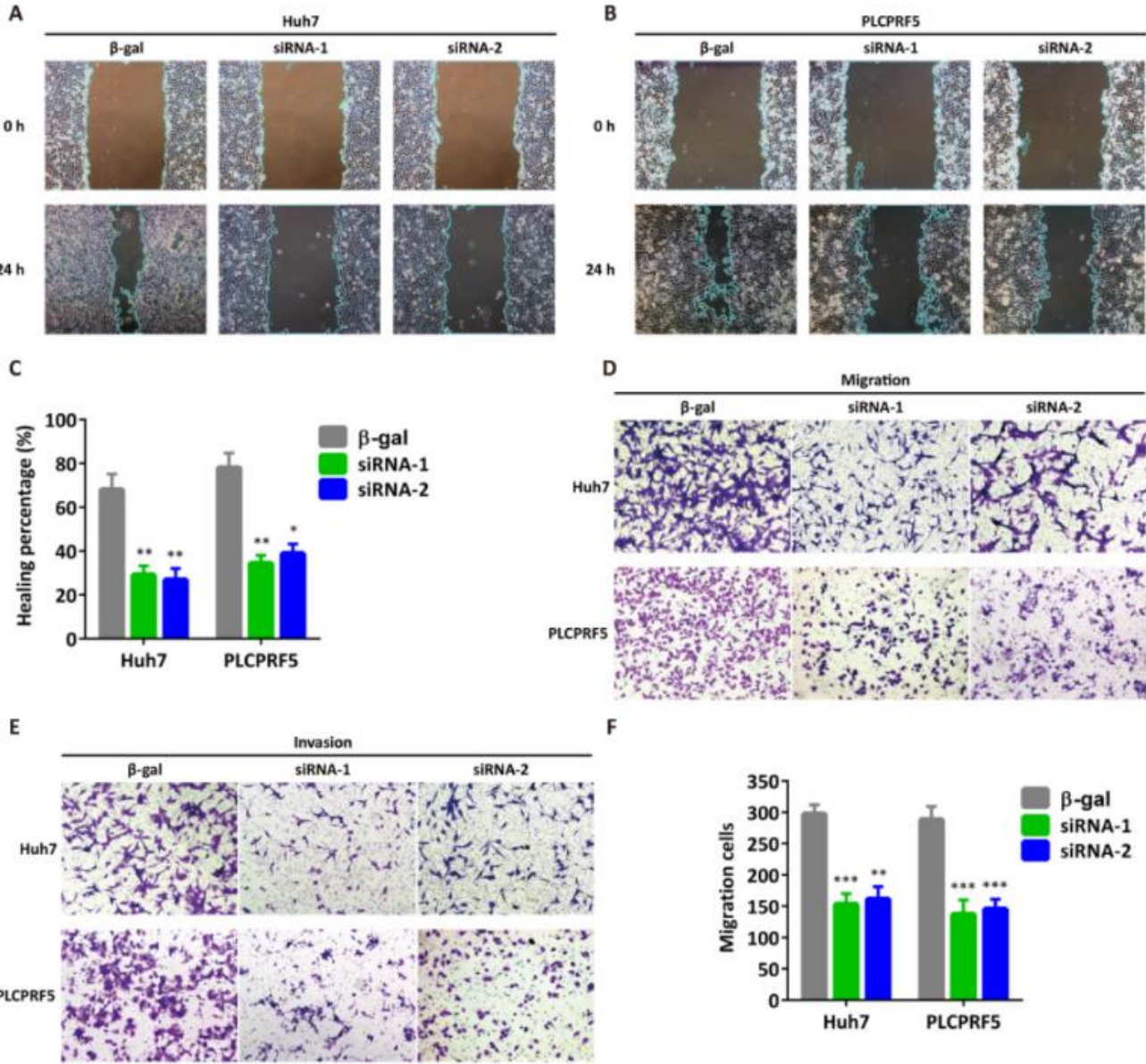


Fig. 4. *In vitro* assessment of the effect of OLFM4 silencing on MMP-7 and E-cadherin.
A. Baseline levels of OLFM4, MMP-7, and E-cadherin expression in Huh7 and PLCPRF5 cell lines. **B.** Effect of transfection of Huh7 and PLCPRF5 cells with siRNA specifically targeting OLFM4 or non-coding siRNA (Beta-gal, 50 nM) for 24 hours on the expression of the indicated molecules after immunoblotting. **C.** Basal expression of OLFM4 in primary

non-tumor hepatocytes isolated from three patients. **D.** Typical pattern of OLFM4 expression at immunofluorescence after transfection with control- or OLFM4-targeting siRNA.



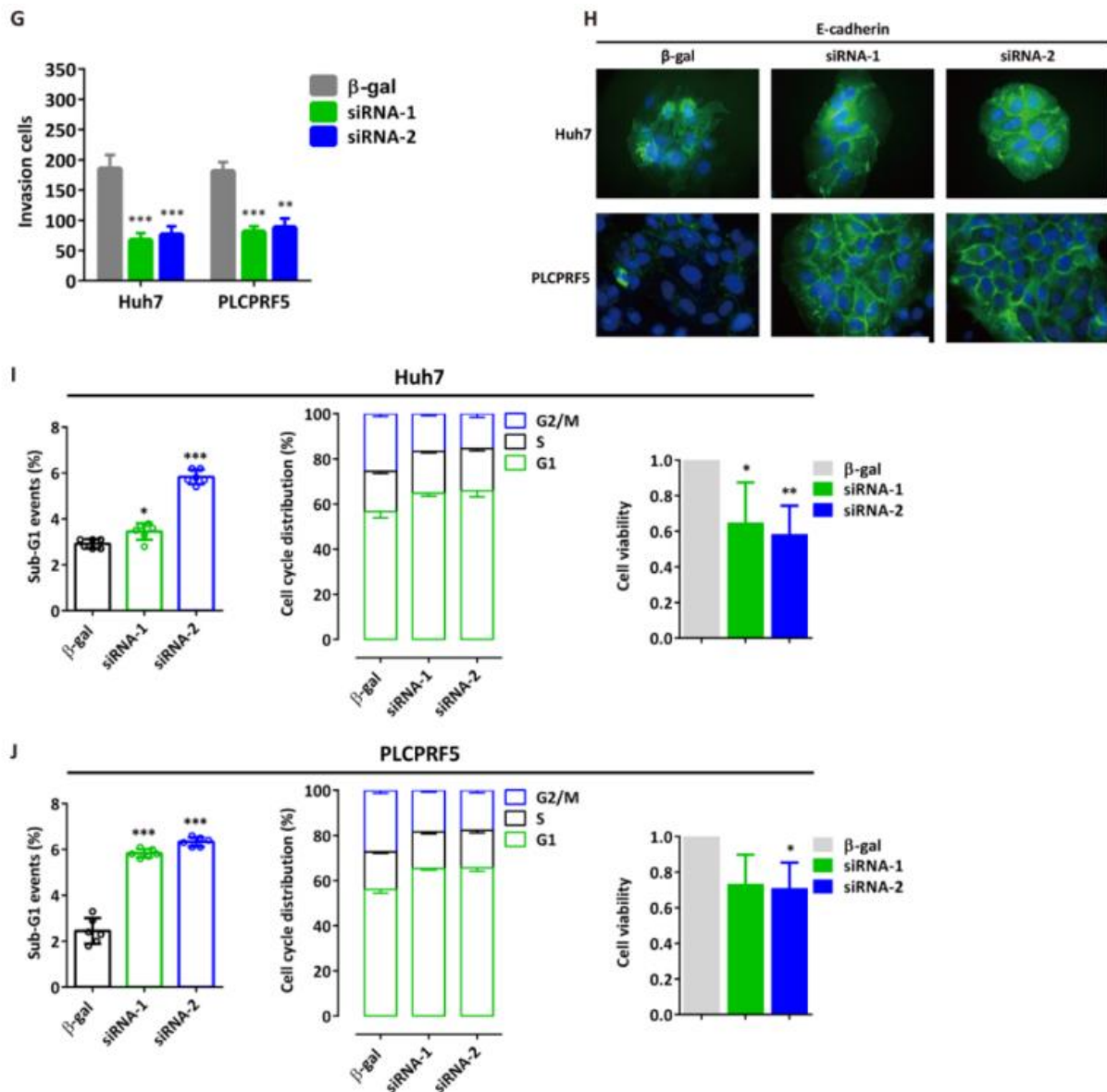


Fig. 5. Effect of OLFM4 silencing on cell migration and invasion. A. B. Assessment of cell motility by wound healing assay in Huh7 or PLCPRF5 cells transfected with siRNA-OLFM4 or control-si-RNA. C. Quantitative analysis of healing area in percentages. D. E. The migration and invasion of Huh7 and PLCPRF5 cells transfected with siRNA-OLFM4 compared with the controls by transwell assay after 24 hours. F. G. Quantitative analysis of migration and invasion cells. H. The E-cadherin expression of Huh7 and PLCPRF5 cells transfected with siRNA-OLFM4 compared with the controls by immunofluorescence after 24 hours. I-J: Effects of OLFM4-silencing by siRNA on sub-G1 events, cell cycle distribution,

and cell viability in Huh7 (I) and PLCPRF5 (J) cell lines. Values represented mean \pm SD from three independent experiments. * $P < 0.05$, ** $P < 0.01$, *** $P < 0.001$, Student's t -test.

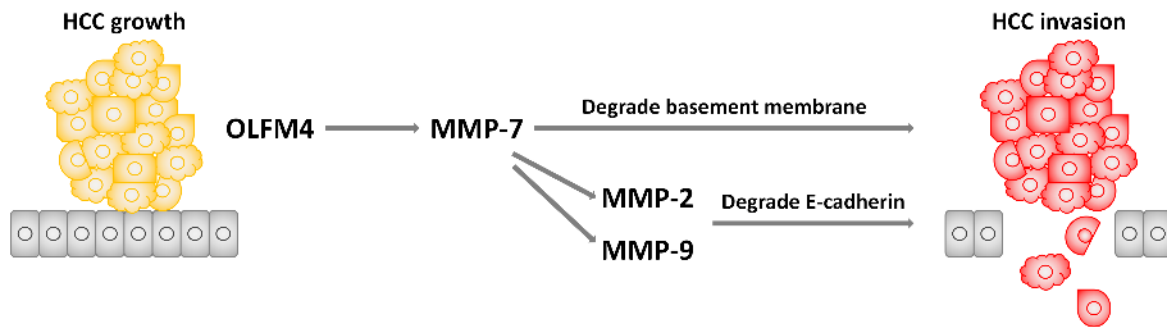


Fig. 6. Schematic diagram describing the hypothesized effect of OLFM4, MMP family members and on invasion and metastasis formation in HCC.

TABLES

Table 1. Summary of clinical and pathologic features.

Feature	Patient count	
	N	%
Age at diagnosis (y)		
< 60	70	44.6
≥ 60	87	55.4
Sex		
Male	122	77.7
Female	35	22.3
Etiology		
HCV	42	26.8
HBV	16	10.1
Toxic/metabolic	92	58.6
Unknown	7	4.5
Severe fibrosis/cirrhosis		
< 5	64	40.8
≥ 5	88	56.0
Not available	5	3.2
Steatosis		
0	65	41.4
1 - 3	87	55.4
Not available	5	3.2
Portal inflammation		
0 - 2	71	45.2
3 - 4	81	51.6
Not available	5	3.2
Piecemeal necrosis		
0 - 2	119	75.8
3 - 4	33	21.0
Not available	5	3.2

Lobular inflammation		
0 - 1	113	72
2 - 3	39	24.8
Not available	5	3.2
Tumor size (cm)		
< 5	81	51.6
≥ 5	76	48.4
Extrahepatic metastasis		
No	151	96.2
Yes	6	3.8
Grading		
1	29	18.5
2	81	51.6
3	33	21.0
Not available	14	8.9
Blood vessel invasion		
No	122	77.1
Yes	35	22.9
Multifocal lesions		
No	106	67.5
Yes	47	29.9
Not available	4	2.5
E-cadherin		
0 - 1	21	13.4
2 - 3	132	84.1
Not available	4	2.5
MMP-7		
0 - 1	27	17.2
2 - 3	129	82.2
Not available	1	0.6
Treatment		
Liver transplantation	56	35.7

Partial hepatectomy 101 64.3

Table 2. Correlation between OLFM4 staining and clinicopathologic parameters in HCC cells.

Feature	Cytoplasm staining		<i>P</i>
	Negative, N (%)	Positive, N (%)	
Age at diagnosis (y)			
< 60	11 (7.0)	59 (37.6)	0.316
≥ 60	9 (5.7)	78 (49.7)	
Sex			
Male	13 (8.3)	109 (69.4)	0.144
Female	7 (4.5)	28 (17.8)	
Etiology			
HCV	4 (2.7)	38 (25.3)	0.684
HBV	2 (1.4)	14 (9.3)	
Toxic/metabolic	14 (9.3)	78 (52.0)	
Severe fibrosis/cirrhosis			
< 5	11 (7.2)	53 (34.9)	0.232
≥ 5	9 (5.9)	79 (52.0)	
Steatosis			
0	13 (8.6)	52 (34.2)	0.05
1 - 3	7 (4.6)	80 (52.6)	
Portal inflammation			
0 - 2	8 (5.6)	63 (41.4)	0.633
3 - 4	12 (7.9)	69 (45.4)	
Piecemeal necrosis			
0 - 2	16 (10.5)	103 (67.8)	0.842
3 - 4	4 (2.6)	29 (19.1)	
Lobular inflammation			
0 - 1	7 (4.6)	106 (69.7)	< 0.001*
2 - 3	13 (8.6)	26 (17.1)	

Tumor size (cm)				
< 5	10 (6.4)	71 (45.2)		0.879
≥ 5	10 (6.4)	66 (42.0)		
Extrahepatic metastasis				
No	18 (11.5)	133 (84.7)		0.169 [¶]
Yes	2 (1.3)	4 (2.5)		
Grading				
G1	2 (1.4)	27 (18.9)		0.367 [¶]
G2 and G3	18 (12.6)	96 (67.1)		
Blood vessel invasion				
No	19 (12.1)	103 (65.6)		0.048 ^{*¶}
Yes	1 (0.6)	34 (21.7)		
Multifocal lesions				
No	15 (9.8)	91 (59.5)		0.552
Yes	5 (3.2)	42 (27.5)		
E-cadherin				
0 - 1	3 (1.9)	18 (11.8)		0.74
2 - 3	17 (11.1)	115 (75.2)		
MMP-7				
0 - 1	9 (5.8)	18 (11.5)		0.002 ^{*¶}
2 - 3	11 (7.1)	118 (75.6)		

Feature	Membrane staining		<i>P</i>
	Negative, N (%)	Positive, N (%)	
Age at diagnosis (y)			
< 60	28 (17.8)	42 (26.8)	0.680
≥ 60	32 (20.4)	55 (35.0)	
Sex			
Male	45 (28.7)	77 (49.0)	0.522
Female	15 (9.6)	20 (12.7)	
Etiology			

HCV	21 (14.0)	21 (14.0)	
HBV	7 (4.7)	9 (6.0)	0.236
Toxic/metabolic	32 (21.3)	60 (40.0)	
Severe fibrosis/cirrhosis			
< 5	27 (17.8)	37 (24.3)	
≥ 5	33 (21.7)	55 (36.2)	0.559
Steatosis			
0	31 (20.4)	34 (22.4)	
1 - 3	28 (18.4)	59 (38.8)	0.052
Portal inflammation			
0 - 2	22 (14.5)	49 (32.2)	
3 - 4	36 (23.7)	45 (29.6)	0.088
Piecemeal necrosis			
0 - 2	48 (31.6)	71 (46.7)	
3 - 4	11 (7.2)	22 (14.5)	0.456
Lobular inflammation			
0 - 1	43 (28.3)	70 (46.1)	
2 - 3	14 (9.2)	25 (16.4)	0.811
Tumor size (cm)			
< 5	34 (21.7)	47 (29.9)	
≥ 5	26 (16.6)	50 (31.8)	0.317
Extrahepatic metastasis			
No	59 (37.6)	92 (58.6)	
Yes	1 (0.6)	5 (3.2)	0.408 [†]
Grading			
G1	13 (9.2)	16 (11.1)	
G2 and G3	39 (27.3)	75 (52.4)	0.289
Blood vessel invasion			
No	45 (28.7)	77 (49.0)	
Yes	15 (9.6)	20 (12.7)	0.522
Multifocal lesions			
No	42 (27.5)	64 (41.8)	0.686

	Yes	17 (11.1)	30 (19.6)	
E-cadherin				
	0 - 1	12 (7.8)	9 (5.9)	0.042*
	2 - 3	45 (29.4)	87 (56.9)	
MMP-7				
	0 - 1	16 (10.3)	11 (7.0)	0.015*
	2 - 3	44 (28.2)	85 (54.5)	

*, statistical significance; ¶, Fisher’s exact test. All other *P* values were calculated by Pearson’s Chi-square test.

Table 3. Cox regression of univariate analyses for OLFM4 staining in HCC tissues.

Parameter	HR	95% CI	<i>P</i>
Age at diagnosis (y)			
< 60			
≥ 60	0.946	0.624 - 1.434	0.795
Sex			
Male			
Female	1.084	0.669 - 1.755	0.743
Etiology			
HCV			
HBV	1.001	0.459 - 2.183	0.998
Toxic/metabolic	1.085	0.659 - 1.787	0.747
Severe fibrosis/cirrhosis			
< 5			
≥ 5	1.286	0.844 - 1.958	0.242
Steatosis			
0			
1 - 3	0.725	0.473 - 1.111	0.140
Portal inflammation			

0 - 2				
3 - 4	1.202	0.787 - 1.835	0.395	
Piecemeal necrosis				
0 - 2				
3 - 4	1.580	0.966 - 2.584	0.068	
Lobular inflammation				
0 - 1				
2 - 3	0.702	0.434 - 1.133	0.148	
Tumor size (cm)				
< 5				
≥ 5	0.950	0.617 - 1.462	0.815	
Extrahepatic metastasis				
No				
Yes	1.186	0.432 - 3.251	0.741	
Grading				
1				
2	0.719	0.424 - 1.219	0.220	
3	1.179	0.658 - 2.112	0.580	
Blood vessel invasion				
No				
Yes	1.879	1.181 - 2.989	0.008*	
Multifocal lesions				
No				
Yes	1.150	0.727 - 1.820	0.549	
E-cadherin				
0 - 1				
2 - 3	0.623	0.342 - 1.137	0.123	
MMP-7				
0 - 1				
2 - 3	1.028	0.590 - 1.790	0.923	
Cytoplasm staining				
Negative				

Positive	2.226	1.186 - 4.177	0.013*
Membrane staining			
Negative			
Positive	1.216	0.781 - 1.891	0.386

*, statistical significance. HR, hazard ration. CI, confidence interval.

Table 4. Cox regression of multivariate analyses for OLFM4 staining in HCC tissues.

Parameter	HR	95% CI	P
Blood vessel invasion			
No			
Yes	1.791	1.124 - 2.854	0.014*
Cytoplasm staining			
Negative			
Positive	2.135	1.135 - 4.015	0.019*

*, statistical significance. HR, hazard ration. CI, confidence interval.

REFERENCES

- 1 Ye, L. *et al.* The PI3K inhibitor copanlisib synergizes with sorafenib to induce cell death in hepatocellular carcinoma (HCC). *Z Gastroenterol* **56**, G3, doi:10.1055/s-0038-1648607 (2018).
- 2 Ye, L. *et al.* Expression, cellular distribution, and prognostic relevance of olfactomedin 4 in hepatocellular carcinoma. *Z Gastroenterol* **56**, KV 300, doi:10.1055/s-0038-1668938 (2018).
- 3 Global, regional, and national disability-adjusted life-years (DALYs) for 333 diseases and injuries and healthy life expectancy (HALE) for 195 countries and territories, 1990-2016: a systematic analysis for the Global Burden of Disease Study 2016. *Lancet (London, England)* **390**, 1260-1344, doi:10.1016/s0140-6736(17)32130-x (2017).
- 4 Jemal, A. *et al.* Annual Report to the Nation on the Status of Cancer, 1975-2014, Featuring Survival. *Journal of the National Cancer Institute* **109**, doi:10.1093/jnci/djx030 (2017).
- 5 Llovet, J. M. *et al.* Hepatocellular carcinoma. *Nature reviews. Disease primers* **2**, 16018, doi:10.1038/nrdp.2016.18 (2016).
- 6 Forner, A., Llovet, J. M. & Bruix, J. Hepatocellular carcinoma. *Lancet (London, England)* **379**, 1245-1255, doi:10.1016/s0140-6736(11)61347-0 (2012).
- 7 Rimassa, L. & Santoro, A. Sorafenib therapy in advanced hepatocellular carcinoma: the SHARP trial. *Expert review of anticancer therapy* **9**, 739-745, doi:10.1586/era.09.41 (2009).
- 8 Bruix, J. *et al.* Regorafenib for patients with hepatocellular carcinoma who progressed on sorafenib treatment (RESORCE): a randomised, double-blind, placebo-controlled, phase 3 trial. *Lancet (London, England)* **389**, 56-66, doi:10.1016/s0140-6736(16)32453-9 (2017).
- 9 Kudo, M. Lenvatinib May Drastically Change the Treatment Landscape of Hepatocellular Carcinoma. *Liver cancer* **7**, 1-19, doi:10.1159/000487148 (2018).
- 10 El-Khoueiry, A. B. *et al.* Nivolumab in patients with advanced hepatocellular carcinoma (CheckMate 040): an open-label, non-comparative, phase 1/2 dose escalation and expansion trial. *Lancet (London, England)* **389**, 2492-2502, doi:10.1016/s0140-6736(17)31046-2 (2017).
- 11 Abou-Alfa, G. K. *et al.* Cabozantinib (C) versus placebo (P) in patients (pts) with advanced hepatocellular carcinoma (HCC) who have received prior sorafenib: Results from the randomized phase III CELESTIAL trial. *Journal of Clinical Oncology* **36**, 207-207, doi:10.1200/JCO.2018.36.4_suppl.207 (2018).
- 12 Gerbes, A. *et al.* Gut roundtable meeting paper: selected recent advances in hepatocellular carcinoma. *Gut* **67**, 380-388, doi:10.1136/gutjnl-2017-315068 (2018).

- 13 Wilhelm, S. *et al.* Discovery and development of sorafenib: a multikinase inhibitor for treating cancer. *Nature reviews. Drug discovery* **5**, 835-844, doi:10.1038/nrd2130 (2006).
- 14 Rimassa, L. *et al.* Tumor and circulating biomarkers in patients with second-line hepatocellular carcinoma from the randomized phase II study with tivantinib. *Oncotarget* **7**, 72622-72633, doi:10.18632/oncotarget.11621 (2016).
- 15 Kabir, T. D. *et al.* A microRNA-7/growth arrest specific 6/TYRO3 axis regulates the growth and invasiveness of sorafenib-resistant cells in human hepatocellular carcinoma. *Hepatology (Baltimore, Md.)* **67**, 216-231, doi:10.1002/hep.29478 (2018).
- 16 Samarin, J. *et al.* PI3K/AKT/mTOR-dependent stabilization of oncogenic far-upstream element binding proteins in hepatocellular carcinoma cells. *Hepatology (Baltimore, Md.)* **63**, 813-826, doi:10.1002/hep.28357 (2016).
- 17 Schulze, K. *et al.* Exome sequencing of hepatocellular carcinomas identifies new mutational signatures and potential therapeutic targets. *Nature genetics* **47**, 505-511, doi:10.1038/ng.3252 (2015).
- 18 Totoki, Y. *et al.* Trans-ancestry mutational landscape of hepatocellular carcinoma genomes. *Nature genetics* **46**, 1267-1273, doi:10.1038/ng.3126 (2014).
- 19 Schneider, P. *et al.* The novel PI3 kinase inhibitor, BAY 80-6946, impairs melanoma growth in vivo and in vitro. *Experimental dermatology* **23**, 579-584, doi:10.1111/exd.12470 (2014).
- 20 Paul, J. *et al.* Simultaneous Inhibition of PI3Kdelta and PI3Kalpha Induces ABC-DLBCL Regression by Blocking BCR-Dependent and -Independent Activation of NF-kappaB and AKT. *Cancer cell* **31**, 64-78, doi:10.1016/j.ccell.2016.12.003 (2017).
- 21 Liu, N. *et al.* BAY 80-6946 is a highly selective intravenous PI3K inhibitor with potent p110alpha and p110delta activities in tumor cell lines and xenograft models. *Molecular cancer therapeutics* **12**, 2319-2330, doi:10.1158/1535-7163.mct-12-0993-t (2013).
- 22 Elster, N. *et al.* A preclinical evaluation of the PI3K alpha/delta dominant inhibitor BAY 80-6946 in HER2-positive breast cancer models with acquired resistance to the HER2-targeted therapies trastuzumab and lapatinib. *Breast cancer research and treatment* **149**, 373-383, doi:10.1007/s10549-014-3239-5 (2015).
- 23 Chou, T. C. Theoretical basis, experimental design, and computerized simulation of synergism and antagonism in drug combination studies. *Pharmacological reviews* **58**, 621-681, doi:10.1124/pr.58.3.10 (2006).
- 24 Will, M. *et al.* Rapid induction of apoptosis by PI3K inhibitors is dependent upon their transient inhibition of RAS-ERK signaling. *Cancer discovery* **4**, 334-347, doi:10.1158/2159-8290.cd-13-0611 (2014).

- 25 Dietrich, P. *et al.* Wild type Kirsten rat sarcoma is a novel microRNA-622-regulated therapeutic target for hepatocellular carcinoma and contributes to sorafenib resistance. *Gut*, doi:10.1136/gutjnl-2017-315402 (2017).
- 26 Xia, H., Ooi, L. L. & Hui, K. M. MicroRNA-216a/217-induced epithelial-mesenchymal transition targets PTEN and SMAD7 to promote drug resistance and recurrence of liver cancer. *Hepatology (Baltimore, Md.)* **58**, 629-641, doi:10.1002/hep.26369 (2013).
- 27 Fruman, D. A. *et al.* The PI3K Pathway in Human Disease. *Cell* **170**, 605-635, doi:10.1016/j.cell.2017.07.029 (2017).
- 28 Thorpe, L. M., Yuzugullu, H. & Zhao, J. J. PI3K in cancer: divergent roles of isoforms, modes of activation and therapeutic targeting. *Nature reviews. Cancer* **15**, 7-24, doi:10.1038/nrc3860 (2015).
- 29 Xu, Y. *et al.* MicroRNA-122 confers sorafenib resistance to hepatocellular carcinoma cells by targeting IGF-1R to regulate RAS/RAF/ERK signaling pathways. *Cancer letters* **371**, 171-181, doi:10.1016/j.canlet.2015.11.034 (2016).
- 30 Berasain, C. Hepatocellular carcinoma and sorafenib: too many resistance mechanisms? *Gut* **62**, 1674-1675, doi:10.1136/gutjnl-2013-304564 (2013).
- 31 Markham, A. Copanlisib: First Global Approval. *Drugs* **77**, 2057-2062, doi:10.1007/s40265-017-0838-6 (2017).
- 32 Dreyling, M. *et al.* Phosphatidylinositol 3-Kinase Inhibition by Copanlisib in Relapsed or Refractory Indolent Lymphoma. *Journal of clinical oncology : official journal of the American Society of Clinical Oncology* **35**, 3898-3905, doi:10.1200/jco.2017.75.4648 (2017).
- 33 Kim, R. D. *et al.* Phase I dose-escalation study of copanlisib in combination with gemcitabine or cisplatin plus gemcitabine in patients with advanced cancer. *British journal of cancer* **118**, 462-470, doi:10.1038/bjc.2017.428 (2018).
- 34 Doi, T. *et al.* A Phase I study of intravenous PI3K inhibitor copanlisib in Japanese patients with advanced or refractory solid tumors. *Cancer chemotherapy and pharmacology* **79**, 89-98, doi:10.1007/s00280-016-3198-0 (2017).
- 35 Musgrove, E. A., Caldon, C. E., Barraclough, J., Stone, A. & Sutherland, R. L. Cyclin D as a therapeutic target in cancer. *Nature reviews. Cancer* **11**, 558-572, doi:10.1038/nrc3090 (2011).
- 36 Ikeda, M. *et al.* A phase 1b trial of lenvatinib (LEN) plus pembrolizumab (PEM) in patients (pts) with unresectable hepatocellular carcinoma (uHCC). *Journal of Clinical Oncology* **36**, 4076-4076, doi:10.1200/JCO.2018.36.15_suppl.4076 (2018).
- 37 Li, H. *et al.* Programmed cell death-1 (PD-1) checkpoint blockade in combination with a mammalian target of rapamycin inhibitor restrains hepatocellular carcinoma growth

- induced by hepatoma cell-intrinsic PD-1. *Hepatology (Baltimore, Md.)* **66**, 1920-1933, doi:10.1002/hep.29360 (2017).
- 38 Albiges, L. *et al.* Efficacy of targeted therapies after PD-1/PD-L1 blockade in metastatic renal cell carcinoma. *European journal of cancer (Oxford, England : 1990)* **51**, 2580-2586, doi:10.1016/j.ejca.2015.08.017 (2015).
- 39 Bruix, J., Reig, M. & Sherman, M. Evidence-Based Diagnosis, Staging, and Treatment of Patients With Hepatocellular Carcinoma. *Gastroenterology* **150**, 835-853, doi:10.1053/j.gastro.2015.12.041 (2016).
- 40 Forner, A., Reig, M. & Bruix, J. Hepatocellular carcinoma. *Lancet (London, England)* **391**, 1301-1314, doi:10.1016/s0140-6736(18)30010-2 (2018).
- 41 Grover, P. K., Hardingham, J. E. & Cummins, A. G. Stem cell marker olfactomedin 4: critical appraisal of its characteristics and role in tumorigenesis. *Cancer metastasis reviews* **29**, 761-775, doi:10.1007/s10555-010-9262-z (2010).
- 42 Aung, P. P. *et al.* Systematic search for gastric cancer-specific genes based on SAGE data: melanoma inhibitory activity and matrix metalloproteinase-10 are novel prognostic factors in patients with gastric cancer. *Oncogene* **25**, 2546-2557, doi:10.1038/sj.onc.1209279 (2006).
- 43 Conrotto, P. *et al.* Identification of new accessible tumor antigens in human colon cancer by ex vivo protein biotinylation and comparative mass spectrometry analysis. *International journal of cancer* **123**, 2856-2864, doi:10.1002/ijc.23861 (2008).
- 44 Takadate, T. *et al.* Novel prognostic protein markers of resectable pancreatic cancer identified by coupled shotgun and targeted proteomics using formalin-fixed paraffin-embedded tissues. *International journal of cancer* **132**, 1368-1382, doi:10.1002/ijc.27797 (2013).
- 45 Koshida, S., Kobayashi, D., Moriai, R., Tsuji, N. & Watanabe, N. Specific overexpression of OLFM4(GW112/HGC-1) mRNA in colon, breast and lung cancer tissues detected using quantitative analysis. *Cancer science* **98**, 315-320, doi:10.1111/j.1349-7006.2006.00383.x (2007).
- 46 Liu, W., Lee, H. W., Liu, Y., Wang, R. & Rodgers, G. P. Olfactomedin 4 is a novel target gene of retinoic acids and 5-aza-2'-deoxycytidine involved in human myeloid leukemia cell growth, differentiation, and apoptosis. *Blood* **116**, 4938-4947, doi:10.1182/blood-2009-10-246439 (2010).
- 47 Li, S. R., Dorudi, S. & Bustin, S. A. Identification of differentially expressed genes associated with colorectal cancer liver metastasis. *European surgical research. Europaische chirurgische Forschung. Recherches chirurgicales europeennes* **35**, 327-336, doi:10.1159/000070603 (2003).

- 48 Lee, H. J. *et al.* Gene expression profiling of metaplastic lineages identifies CDH17 as a prognostic marker in early stage gastric cancer. *Gastroenterology* **139**, 213-225.e213, doi:10.1053/j.gastro.2010.04.008 (2010).
- 49 Kobayashi, D., Koshida, S., Moriai, R., Tsuji, N. & Watanabe, N. Olfactomedin 4 promotes S-phase transition in proliferation of pancreatic cancer cells. *Cancer science* **98**, 334-340, doi:10.1111/j.1349-7006.2007.00397.x (2007).
- 50 Oue, N. *et al.* Serum olfactomedin 4 (GW112, hGC-1) in combination with Reg IV is a highly sensitive biomarker for gastric cancer patients. *International journal of cancer* **125**, 2383-2392, doi:10.1002/ijc.24624 (2009).
- 51 Besson, D. *et al.* A quantitative proteomic approach of the different stages of colorectal cancer establishes OLFM4 as a new nonmetastatic tumor marker. *Molecular & cellular proteomics : MCP* **10**, M111.009712, doi:10.1074/mcp.M111.009712 (2011).
- 52 Liu, W. *et al.* Reduced hGC-1 protein expression is associated with malignant progression of colon carcinoma. *Clinical cancer research : an official journal of the American Association for Cancer Research* **14**, 1041-1049, doi:10.1158/1078-0432.ccr-07-4125 (2008).
- 53 Kim, K. K., Park, K. S., Song, S. B. & Kim, K. E. Up regulation of GW112 Gene by NF kappaB promotes an antiapoptotic property in gastric cancer cells. *Molecular carcinogenesis* **49**, 259-270, doi:10.1002/mc.20596 (2010).
- 54 Zhang, X., Huang, Q., Yang, Z., Li, Y. & Li, C. Y. GW112, a novel antiapoptotic protein that promotes tumor growth. *Cancer research* **64**, 2474-2481 (2004).
- 55 Liu, W. & Rodgers, G. P. Olfactomedin 4 expression and functions in innate immunity, inflammation, and cancer. *Cancer metastasis reviews* **35**, 201-212, doi:10.1007/s10555-016-9624-2 (2016).
- 56 Kononen, J. *et al.* Tissue microarrays for high-throughput molecular profiling of tumor specimens. *Nature medicine* **4**, 844-847 (1998).
- 57 Kriegl, L. *et al.* Expression, cellular distribution, and prognostic relevance of TRAIL receptors in hepatocellular carcinoma. *Clinical cancer research : an official journal of the American Association for Cancer Research* **16**, 5529-5538, doi:10.1158/1078-0432.ccr-09-3403 (2010).
- 58 Bosman FT, C. F., Hruban R, Theise N. *WHO Classification of Tumours of the Digestive System, ed 4.*, (2010).
- 59 Ishak, K. *et al.* Histological grading and staging of chronic hepatitis. *Journal of hepatology* **22**, 696-699 (1995).
- 60 Kleiner, D. E. *et al.* Design and validation of a histological scoring system for nonalcoholic fatty liver disease. *Hepatology (Baltimore, Md.)* **41**, 1313-1321, doi:10.1002/hep.20701 (2005).

- 61 Thasler, W. E. *et al.* Charitable State-Controlled Foundation Human Tissue and Cell Research: Ethic and Legal Aspects in the Supply of Surgically Removed Human Tissue For Research in the Academic and Commercial Sector in Germany. *Cell and tissue banking* **4**, 49-56, doi:10.1023/a:1026392429112 (2003).
- 62 Lee, S. M., Schelcher, C., Demmel, M., Hauner, M. & Thasler, W. E. Isolation of human hepatocytes by a two-step collagenase perfusion procedure. *Journal of visualized experiments : JoVE*, doi:10.3791/50615 (2013).
- 63 Broutier, L. *et al.* Human primary liver cancer-derived organoid cultures for disease modeling and drug screening. *Nature medicine* **23**, 1424-1435, doi:10.1038/nm.4438 (2017).
- 64 Schneider, M. R. *et al.* Evidence for a role of E-cadherin in suppressing liver carcinogenesis in mice and men. *Carcinogenesis* **35**, 1855-1862, doi:10.1093/carcin/bgu109 (2014).
- 65 Canel, M., Serrels, A., Frame, M. C. & Brunton, V. G. E-cadherin-integrin crosstalk in cancer invasion and metastasis. *Journal of cell science* **126**, 393-401, doi:10.1242/jcs.100115 (2013).
- 66 Jiang, W. G. *et al.* Tissue invasion and metastasis: Molecular, biological and clinical perspectives. *Seminars in cancer biology* **35** Suppl, S244-s275, doi:10.1016/j.semcancer.2015.03.008 (2015).
- 67 Stuelten, C. H., Parent, C. A. & Montell, D. J. Cell motility in cancer invasion and metastasis: insights from simple model organisms. *Nature reviews. Cancer* **18**, 296-312, doi:10.1038/nrc.2018.15 (2018).
- 68 Liu, W., Liu, Y., Li, H. & Rodgers, G. P. Olfactomedin 4 contributes to hydrogen peroxide-induced NADPH oxidase activation and apoptosis in mouse neutrophils. *American journal of physiology. Cell physiology* **315**, C494-c501, doi:10.1152/ajpcell.00336.2017 (2018).
- 69 Wang, X. Y., Chen, S. H., Zhang, Y. N. & Xu, C. F. Olfactomedin-4 in digestive diseases: A mini-review. *World journal of gastroenterology* **24**, 1881-1887, doi:10.3748/wjg.v24.i17.1881 (2018).
- 70 Zhang, J. *et al.* Identification and characterization of a novel member of olfactomedin-related protein family, hGC-1, expressed during myeloid lineage development. *Gene* **283**, 83-93 (2002).
- 71 Tomarev, S. I. & Nakaya, N. Olfactomedin domain-containing proteins: possible mechanisms of action and functions in normal development and pathology. *Molecular neurobiology* **40**, 122-138, doi:10.1007/s12035-009-8076-x (2009).
- 72 Chen, L. *et al.* Olfactomedin 4 suppresses prostate cancer cell growth and metastasis via negative interaction with cathepsin D and SDF-1. *Carcinogenesis* **32**, 986-994, doi:10.1093/carcin/bgr065 (2011).

- 73 Liu, W., Chen, L., Zhu, J. & Rodgers, G. P. The glycoprotein hGC-1 binds to cadherin and lectins. *Experimental cell research* **312**, 1785-1797, doi:10.1016/j.yexcr.2006.02.011 (2006).
- 74 Chin, K. L. *et al.* The regulation of OLFM4 expression in myeloid precursor cells relies on NF-kappaB transcription factor. *British journal of haematology* **143**, 421-432, doi:10.1111/j.1365-2141.2008.07368.x (2008).
- 75 Liu, W., Zhu, J., Cao, L. & Rodgers, G. P. Expression of hGC-1 is correlated with differentiation of gastric carcinoma. *Histopathology* **51**, 157-165, doi:10.1111/j.1365-2559.2007.02763.x (2007).

LIST OF ABBREVIATIONS

AKT	Serine/threonine kinase
ABC	Avidin/biotin
AEC	3-Amino-9-ethylcarbazole
BSA	Bovine serum albumin
CI	Combination index/ Confidence interval
DMEM	Dulbecco's modified eagle medium
DMSO	Dimethyl sulfoxide
DSMZ	Deutsche Sammlung von Mikroorganismen und Zellkulturen
ECL	Enhanced chemiluminescence
EDTA	Ethylenediaminetetraacetic acid
FCS/FBS	Fetal calf/bovine serum
FACS	Fluorescence-activated cell sorting
hGC-1	G-CSF stimulated clone 1
HCC	Hepatocellular carcinoma
H&E	Hematoxylin and eosin
HR	Harzard ration
HTCR	Human tissue and cell research
mTOR	Mammalian target of rapamycin
MMP	Matrix metalloproteinase

MCR	Munich cancer registry
OLFM4	Olfactomedin 4
Opti-MEM	Minimal essential medium
OS	Overall survival
P/S	Penicillin/streptomycin
PBS	Phosphate buffered saline
PI3K	Phosphatidylinositol-3-kinase
PAGE	Polyacrylamide gel electrophoresis
PVDF	Polyvinylidene difluoride
PMSF	Phenylmethanesulfonyl fluoride
PI	Propidium iodide
RIPA	Radio immuno precipitation assay
RT	Room temperature
RPM	Round per minute
SDS	Sodium dodecylsulfate
SD	Standard deviation
SR	Sorafenib resistant
TMA	Tissue microarray
TEMED	Tetramethylethylenediamine
TBS/T	Tris buffered saline with Tween
WHO	World health organization

ACKNOWLEDGMENT

At first, I would like to express my sincere gratitude to my supervisor, PD Dr. Enrico De Toni, for his continuous support, immense knowledge, great passion and endless patience. Although time was always limited for him, he tried to guide me every time when I faced problems either in research or during daily life. As an outstanding doctor and scientist, he is always full of pleasant humour and invincible courage. The most impressive thing I learned from him was the authentic and scientific attitude to conduct research and take care of patients.

Secondly, I want to express my deep thanks to my colleagues in Med II for their unselfish help and cooperation during my whole study. They are doctoral students Jiang Zhang, Hanwei Li, Can and TAs Andreas Ziesch, Andrea Ofner, Ralf, Moni and Ingrid. They taught me patiently and encouraged me a lot. Besides, I would like to say many thanks to Dr. Florian Reiter, he is very kind and helpful. Without his support, I will not be able to participate so many projects in the field of liver fibrosis. Moreover, I also want to express my sincere appreciation to Prof. Dr. Julia Mayerle and Prof. Dr. Alexander L. Gerbes, the chiefs of Med II, for the opportunities to join scientific seminars and international meetings.

Thirdly, I would like to thank the Chinese Scholarship Council (CSC) for its financial support during my doctoral study. Thanks to the LMU – CSC program, I met many friends and had a great time in Munich.

Finally, I want to express thanks to my family, my sister and her husband, my mother and father, and my lovely girlfriend. They love me so much and always support me.

CURRICULUM VITAE

Personal Information

Name: Liangtao Ye

Gender: Male

Date of Birth: 13. 03. 1990

Place of Birth: Shaoguan, Guangdong, China

Nationality: Chinese

Telephone: 0049 (0) 15733603366

E-mail: mdliaogtao@163.com

Address: Allinger Str. 27, 82178, Puchheim, Germany

Education

2008 - 2013: Zhongshan School of Medicine,
Sun Yat-sen University,
Guangzhou, China
Specialty: Clinical Medicine
Degree: Bachelor in Medicine

2013 - 2016: Sun Yat-sen Memorial Hospital,
Sun Yat-sen University,

Guangzhou, China

Specialty: Hepatopancreatobiliary Surgery

Degree: Master in Medicine

2016 - 2019:

Liver Center Munich,

Department of Medicine II,

Klinikum der Universität München,

Ludwig-Maximilians-Universität München

Specialty: Hepatology, Doktorand

Funding

‘Investigation of the PI3K/AKT pathway inhibitor copanlisib in combination with sorafenib in gastroenterologic tumors’.

K. L. Weigand'sche Stiftung, Ludwig-Maximilians-Universität München.
Finanzstelle 80733078.

Abstracts

1. **L Ye**, J Mayerle, A Ziesch, K Wei, AL Gerbes, EN De Toni. The PI3K inhibitor copanlisib synergizes with sorafenib to induce cell death in hepatocellular carcinoma (HCC). *Z Gastroenterol* 2018; 56(05): e22.

Poster. 46. Jahrestagung der Gesellschaft für Gastroenterologie in Bayern e.V. (GFGB), Munich, June 14th – 16th, 2018.

2. **L Ye**, L Brandl, J Mayerle, T Kirchner, AL Gerbes, EN De Toni. Expression, cellular distribution, and prognostic relevance of olfactomedin 4 in hepatocellular carcinoma. *Z Gastroenterol* 2018; 56(08): e308.

Oral presentation. 73. Jahrestagung der Deutschen Gesellschaft für Verdauungs- und Stoffwechselkrankheiten mit Sektion Endoskopie (DGVS), Munich, September 12nd – 15th, 2018.

3. FP Reiter, **L Ye**, F Bösch, R Wimmer, R Artmann, A Ziesch, V Kanitz, D Mayr, M Trauner, I Regel, AL Gerbes, J Mayerle, S Hohenester, E de Toni, G Denk. Akalzämische Vitamin-D-Analoga zeigen antifibrotische Effekte *in vitro* in hepatischen Sternzellen und *in vivo* im CCl₄-Mausmodell. *Z Gastroenterol* 2019; 57(01): e22.

Poster. 35. Jahrestagung der Deutschen Arbeitsgemeinschaft zum Studium der Leber GASL, Heidelberg, February 22nd – 23rd, 2019.

4. FP Reiter, **L Ye**, F Bösch, R Wimmer, R Artmann, A Ziesch, V Kanitz, D Mayr, M Trauner, I Regel, AL Gerbes, J Mayerle, S Hohenester, E de Toni, G Denk. Alcalcemic vitamin D analogues show antifibrotic effects *in vitro* while paricalcitol prevents progression of established fibrosis in the CCl₄ mouse-model. *JOURNAL OF HEPATOLOGY* (Vol. 70, pp. E200-E201).

Poster. EASL The International Liver Congress™, Vienna, Austria, April 10th – 14th, 2019.

5. FP Reiter, G Denk, A Ziesch, A Ofner, R Wimmer, S Hohenester, M Spampatti, **L Ye**, AL Gerbes, J Mayerle, EN De Toni. Die Verwendung des CDK 4/6 Inhibitors Ribociclib – ein erster biomarkerbasierter Therapieansatz für die Behandlung des HCC? Z Gastroenterol 2018; 56(08): e315.

Oral presentation. 73. Jahrestagung der Deutschen Gesellschaft für Verdauungs- und Stoffwechselkrankheiten mit Sektion Endoskopie (DGVS), Munich, September 12nd – 15th, 2018.

6. FP Reiter, G Denk, A Ziesch, A Ofner, R Wimmer, S Hohenester, M Spampatti, **L Ye**, AL Gerbes, J Mayerle, EN De Toni. Ribociclib Exerts Antitumoral Effects in HCC Cells with High Retinoblastoma-Protein Expression. Hepatology, Volume 68, No. 1 (Suppl).

Presidential Poster of Distinction (Top 10%). The Liver Meeting® 2018, American Association for the Study of Liver Diseases (AASLD), San Francisco, November 9th – 13rd, 2018.

Publications

1. **Ye L**, Mayerle J, Ziesch A, et al. The PI3K inhibitor copanlisib synergizes with sorafenib to induce cell death in hepatocellular carcinoma (HCC). Cell death discovery 5.1 (2019): 86.

2. **Ye L,** Brandl L, Reiter FP, et al. Prognostic significance and functional relevance of olfactomedin 4 (OLFM4) in early-stage hepatocellular carcinoma (HCC). *Clinical and Translational Gastroenterology* (Under review)

3. Reiter FP, **Ye L,** et al. Antifibrotic effects of acalcemic vitamin D analogues in murine and human hepatic stellate cells and in the CCl4 mouse model. *Laboratory Investigation* (Minor revision)

4. Reiter FP, Denk G, Ziesch A, Ofner A, Wimmer R, Hohenester S, Spampatti M, **Ye L,** et al. Predictors of ribociclib-mediated antitumoral effects in native and sorafenib-resistant human hepatocellular carcinoma cells. *Cellular Oncology* (Accepted)

5. **Ye L,** Ye H, Zhou Q, et al. A retrospective cohort study of pancreatic neuroendocrine tumors at single institution over 15 years: New proposal for low-and high-grade groups, validation of a nomogram for prognosis, and novel follow-up strategy for liver metastases[J]. *International Journal of Surgery*, 2016, 29: 108-117.

6. **叶良涛,**周泉波, 叶会霖, 等. 肿瘤相关巨噬细胞和 KIT 评估胰腺神经内分泌肿瘤肝转移及预后的价值[J]. *中华胰腺病杂志*, 2016 (05): 314-319.

7. 周泉波, 叶良涛, 李国林, 等. 胰管结石合并胰腺癌的诊治分析 (附 9 例报道)[J]. 中国普外基础与临床杂志, 2016, 23(6): 663-666.
8. 叶会霖, 叶良涛, 周雨, 等. 肿瘤相关巨噬细胞通过 PI3K/Akt 途径促进胰腺癌浸润迁移的研究[J]. 中华普通外科学文献 (电子版), 2015, 9(3): 23-27.
9. 伍志辉, 林青, 叶良涛, 等. 球蛋白/胆碱脂酶比值在评估肝储备功能中的作用[J]. 岭南现代临床外科, 2014 (3): 18.
10. Ye H, Zhou Q, Zheng S, Li G, Lin Q, Ye L, et al. FEZF1-AS1/miR-107/ZNF312B axis facilitates progression and Warburg effect in pancreatic ductal adenocarcinoma[J]. Cell death & disease, 2018, 9(2): 34.
11. Liu G, Zhu J, Yu M, Cai C, Zhou Y, Yu M, Fu Z, Gong Y, Yang B, Li Y, Zhou Q, Lin Q, Ye H, Ye L, et al. Glutamate dehydrogenase is a novel prognostic marker and predicts metastases in colorectal cancer patients[J]. Journal of translational medicine, 2015, 13(1): 144.
12. Zheng S, Chen H, Wang Y, Gao W, Fu Z, Zhou Q, Jiang Y, Lin Q, Tan L, Ye H, Zhao X, Luo Y, Li G, Ye L, et al. Long non-coding RNA LOC389641 promotes progression of pancreatic ductal adenocarcinoma and increases cell

invasion by regulating E-cadherin in a TNFRSF10A-related manner[J]. *Cancer letters*, 2016, 371(2): 354-365.

13. Lao X M, Luo G, **Ye L T**, et al. Effects of antiviral therapy on hepatitis B virus reactivation and liver function after resection or chemoembolization for hepatocellular carcinoma[J]. *Liver International*, 2013, 33(4): 595-604.